THESIS

INVESTIGATING THE ROLE OF THE CELLULAR RNA DECAY PATHWAY DURING FLAVIVIRUS REPLICATION

Submitted by

Denis

Department of Microbiology, Immunology, and Pathology

In partial fulfillment of the requirements

For the Degree of Master of Science

Colorado State University

Fort Collins, Colorado

Fall 2022

Master's Committee:

Advisor: Brian Geiss

Jeffrey Wilusz
Gregory Ebel
Christopher Snow

ABSTRACT

INVESTIGATING THE ROLE OF THE CELLULAR RNA DECAY PATHWAY DURING FLAVIVIRUS REPLICATION

The Cellular RNA decay pathway is an important regulatory system that affects both the quality and quantity of mRNA within the cells. Previous studies have shown that RNA viruses develop evasion mechanism to the cellular RNA decay pathway due to its antiviral nature. In eukaryotic cells, 5'-3' exonucleolytic decay mediated by XRN1 is known to be the major RNA decay pathway that interacts with RNA viruses. To provide RNA substrates for XRN1 degradation, cellular mRNA and viral RNA need to be processed by decapping enzymes such as DXO and DCP2 or RNA triphosphatases such as DUSP11 and NUDT2. Currently, there are few studies that have examined the roles of these proteins during RNA virus replication. In this study, we performed a loss-of-function experiment utilizing siRNA-mediated knockdown to reduce various RNA decay proteins and examine their effects on flavivirus replication. Collectively, our data suggested that knocking down DUSP11 and NUDT2 did not significantly affect the replication of infectious flaviviruses, whereas depletion of DCP2, showed significantly diminished West Nile virus and Zika virus replication but not on yellow fever virus. The results of this project indicate that DCP2 acts as a proviral factor for several but not all flaviviruses during infection and provide new insight into how flaviviruses may generate RNAs for XRN1-mediated degradation and subsequent XRN1 inhibition.

ACKNOWLEDGEMENTS

First and foremost, I would like to express my gratitude to my advisor, Dr. Brian Geiss, for his never-ending support and guidance towards the course of my master studies. I learn a lot on how to become better scientist and to always look at the bigger picture. I would also extend my gratitude to Fulbright M.A Scholarship program and American Indonesian Exchange Foundation (AMINEF). Thank you for trusting me with the scholarship position and belief that I have what it takes to complete the program. Special thanks to Loran Anderson for helping me these past few months and Geiss lab members: Dr. Michael Mingroni (for providing me RNA samples and virus stocks to work with!), James Terry, Kristen Denale, Lauren Malsick, Brooke Enney, Amanda Bartels, and Marina Fujii. You guys are always there to support me scientifically and personally.

Thank you to the lab of Dr. Rushika Perrera for providing the Huh7 cells that were used extensively in this study. I would also like to thank John Anderson for answering all my questions regarding to RNA work. A big "Thank You!" to all my committee members, Dr. Jeffrey Wilusz, Dr. Gregory Ebel, and Dr. Christopher Snow for all the valuable feedbacks during the committee meeting.

Thank you to my parents and sister, Yohanes Jong, Jetyana Susantyo, and Laurensia Laura for being understanding and supporting me everytime. Also thank you to all my friends in Indonesia, as they are one of the biggest sources of comfort for me during my graduate journey here at CSU. Lastly, thank you to Mark Windyka, for always being there and supporting me whenever I need encouragement.

TABLE OF CONTENTS

LIST OF FIGURES

INTRODUCTION

1. Flaviviruses: an emerging threat and global public health problem

Mosquito-borne diseases are a major public health problem throughout the world. These mosquito-borne pathogens such as dengue, Zika, and West Nile viruses infect millions of people annually and cause a significant mortality and morbidity in human and animal populations. Efforts to control and treat these diseases have also caused a significant global economic burden (1). The most prominent agents of mosquito-borne pathogens are viruses, particularly those that belong to the Flavivirus genera. Over the past decades, a particular flavivirus known as dengue virus (DENV) has caused a globalized outbreak and accounts for 400 million cases annually with developing and poor countries suffering the most from this epidemic (2). Although DENV infection accounts for most of the Flavivirus outbreak, other flavivirus such as West Nile virus (WNV) and Zika virus (ZIKV) have also caused significant mortality and morbidity in the population. The lack of public health infrastructure and human mobilization have been thought to be the main cause of the globalization of these diseases. Additionally, climate change is expected to increase mosquitoes activity and spread them to new geographic regions as the temperature becomes warmer and more suitable for the mosquitoes (3). Considering these two factors, mosquito-borne flavivirus outbreaks are expected to increase in the future with more countries and people being affected. Currently, there are limited treatment options for any flaviviral disease, which is predominately supportive care. Moreover, although vector control through chemical and biological measures is on-going, insecticide resistance towards chemical control agents is readily observed and biological control systems, including *Wolbachia* look promising at first but their long term evolutionary effect on the viruses still need to be monitored

(4,5). Therefore, it is important to expand existing treatment options to mitigate the impact of these diseases on vulnerable populations.

2. Different disease caused by Flaviviruses

West Nile virus (WNV) is one of the biggest arboviral disease threats that is endemic in North America but is also found globally throughout Asia, Africa, and South America (6). Currently, WNV infections have been reported in 48 states in America and are correlated with the distribution of its mosquito vector, *Culex pipiens* (7). The infection cycle occurs with avian hosts as the primary virus reservoirs that transmit to *Culex* mosquitoes when taking a bloodmeal, with WNV transmitted incidentally to humans through subsequent mosquito bites. WNV can be neuroinvasive by gaining access to the brain through several mechanisms, which manifest as meningitis, encephalitis, and/or acute flaccid paralysis (8). Most WNV infections resolve on their own and only around 25% developed into mild WNV fever. However, around 1% of WNV infection cases show prolonged symptoms such as extreme fatigue and, in patients with neuroinvasive pathology, the fatality rate is approximately 10% (9). Treatments for WNV infection have only been supportive care and is difficult to assess their efficacy of due to the variable outcomes of WNV infection. Efforts to prevent WNV infection by controlling the mosquito population, using insecticides such as DEET, IR3535, and picaridin, have been employed due to their safety and efficacy profiles. However, insecticide resistance has been detected in *Culex* vectors, which can diminish the effectiveness of the mosquito control regimen (10). Additionally, *Wolbachia*, a bacteria under consideration as a future vector control technique, has also been shown to enhance WNV replication inside the mosquito's gut (11),

raising questions about its utility. Therefore, providing an effective treatment against WNV will be pivotal to winning the ongoing war against WNV.

Zika virus (ZIKV) is a mosquito-borne flavivirus that has caused major concern in pregnant women due to its potential for causing birth defects in fetuses. The virus was first identified in the Zika Forest in Uganda in 1947. Since then, the virus has spread locally and detected serologically in multiple African countries such as Nigeria, Senegal, Egypt, Kenya, amongst others (12). From Africa, ZIKV spread to Southeast Asia, as demonstrated by ZIKV antibodies detection found in Thailand, Vietnam, Malaysia, and Indonesia (13). ZIKV continued to be transmitted to the equatorial belt and in 2007, an outbreak of ZIKV was reported in Yap Island, Micronesia. This marked the first detection of ZIKV outside of Africa and Asia. In 2013-2014, another ZIKV outbreak was identified in French Polynesia. Although most of the patients showed mild symptoms, the first case of Guillain-Barre syndrome (GBS) was reported in one patient and, interestingly, the incidence of GBS was estimated to be ~20 fold higher in the French Polynesia ZIKV outbreak where DENV and chikungunya virus were co-circulating at the same time (14). In 2015, the first ZIKV infection was reported in South America, in the country of Brazil. During this outbreak, the first congenital and microcephaly cases associated with ZIKV infection were also reported (15,16). ZIKV epidemiology is somewhat complicated as ZIKV is not solely transmitted by *Aedes* mosquitoes, but can also use sexual transmission, maternal to fetal transmission, and blood transfusion routes (17,18), making prediction of viral spread globally very challenging.

ZIKV has historically been understudied due to its localized outbreaks and mild symptoms. However, the serious complications involving pregnant women and birth defects first seen in 2015 fostered more studies to better understand the pathology of the virus (19). Fetal birth defects are mediated through transplacental transmission of ZIKV (from mother to the fetus), and invasion of ZIKV in fetal neural and ocular progenitor cells can result in spontaneous abortion, brain deformities or microcephaly (20). Additionally, ZIKV infection has been shown to trigger Guillain-Barre Syndrome, a rare clinical presentation where the host immune system attacks self-neurons and causes neurological symptoms such as paralysis and muscle weakness (21). To date, no treatment is available for ZIKV infection and research is focusing more on designing an effective vaccine to prevent infection. Currently, Zika virus vaccines are in development using multiple platforms such as live-attenuated, recombinant viral vectors based, mRNA-based, and subunit protein based (22). Although multiple vaccines are in development, it will take years before any vaccine is available due to the lengthy clinical trial and drug approval process. Furthermore, flavivirus antibody response has been known to elicit cross-reactivity that can cause antibody-dependent enhancement (ADE) that induces a major inflammatory response (23), similar to what is observed with DENV infections. In a study that was published by Katzelnick et.al, prior ZIKV infection increases the probability of symptomatic DENV-2 infection (24). This finding presents serious complications to the current monovalent ZIKV vaccine approaches in development and whether they can be safely administered in individuals with no prior DENV infection history.

Yellow fever virus (YFV) is a mosquito-borne flavivirus that is transmitted by *Aedes* mosquitoes, the same vectors that can transmit chikungunya, dengue, and Zika viruses. Most infection resulted in mild symptoms such as fever, chills, headache, and muscle ache. However,

in 15% of the cases, severe symptoms such as jaundice, bleeding, shock, organ failure, and death can occur. In severe cases, organ failure is caused by uncontrolled production of inflammatory cytokines known as the cytokine storm (25). To prevent yellow fever virus infection, a live attenuated vaccine was developed in 1937 at the Rockefeller Institute. The vaccine was produced by passaging the Asibi and French strains of YFV in both mouse and chicken embryo. Upon passaging it 100 times in the nervous tissue of chick embryos, the virus acquired an attenuating mutation when injected into mice, the attenuated virus failed to cause a disease. This vaccine strain of YFV was named 17D (26). The vaccine is now used as a travel requirement to countries where yellow fever is endemic. Vaccine efficacy is sufficient in producing neutralizing antibodies close to full protection after one month. However, waning antibody has been reported in the pediatric population, alerting local public health authorities to consider whether booster administration is needed (27). Vaccine failures have also been reported in several studies with no clear evidence of the cause. Several explanations were proposed such as waning antibodies, infection by the sylvatic strain of the virus, or underlying medical history of the patients (28). Additionally, persons in susceptible populations who are pregnant women, immunocompromised individuals, or have egg allergies are unable to receive the vaccination (29). Considering these facts, developing a treatment for YFV is necessary to provide a way to help these vulnerable groups.

3. The molecular biology of flaviviruses: replication and genome structure

To create an effective treatment against flavivirus, a better understanding about flavivirus replication mechanisms and its genome structure are needed. Flavivirus replication starts by entry of the virus particle into the cells through receptor-mediated endocytosis (Fig 1). Receptors

that have been associated with Flavivirus infection include the innate immune receptor DC-SIGN (WNV & ZIKV), mannose, glycosaminoglycans, transmembrane TIM-1, TAM, and entry of the virus is mediated through clathrin mediated endocytosis (30). Upon receptor binding, the virus particle is internalized into cellular endosomes. Inside the endosomes, acidification causes a conformational change in the viral envelope protein that induces fusion of the viral and endosomal membranes, releasing the capsid and viral genome into the cytoplasm (31). The viral RNA genome is then trafficked to the endoplasmic reticulum (ER) where it will be translated by the host's ribosome on the rough endoplasmic reticulum (RER) (32). During translation, a transmembrane viral polyprotein is produced which is subsequently cleaved by NS3 viral protease into mature viral proteins (33). Once cleaved, multiple non-structural proteins such as NS1, NS2A, NS2B, NS4A, and NS4B initiate the formation of the replication compartment in the ER (34). Viral RNA genome production is then carried out inside the replication compartment. From its single-stranded positive-sense RNA genome, intermediate single-stranded negative-sense RNA is produced by the NS5 viral polymerase. The negative-sense RNA is then used as the template to produce more 5' capped single stranded positive sense RNA genomes. The newly synthesized viral genome is packaged by capsid proteins and buds into the ER to obtain its envelope, forming immature virions. These immature virions travel into the Golgi apparatus where the viral envelope protein is cleaved by the cellular furin protease prior to release. The cleaved viral envelope protein allows the virus particle to exit the cells via exocytosis where it can travel and infect neighboring cells.

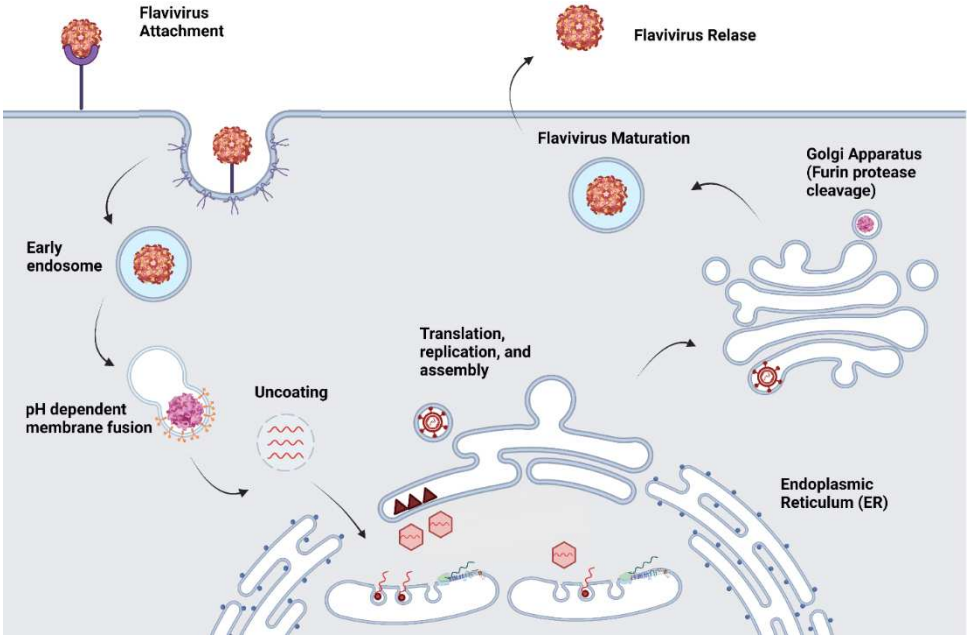

Fig. 1 ***Flavivirus life cycle and replication within infected cells.*** Flavivirus entry into the cells is mediated through endocytosis forming early endosome. Change in pH promotes membrane fusion of endosome and uncoating of viral genome. Viral genome is then undergoing translation, replication, and assembly in ER before further matured in golgi apparatus. Matured flavivirus is then released outside of the cells through exocytosis. Image generated by BioRender.

3.1 Flavivirus 5' UTR and cap structure

The Flavivirus genome have been the subject of research for decades. The flavivirus genome consisted of cap structure (N7-Gppp and 2'O methylated at the first nucleotide of the 5'UTR) (Fig.2). The 5'cap structure functions as a translation initiation factor that will recruit the host translation initiation factors and ribosomes to synthesize viral proteins. In addition, the 5' cap also helps to stabilize the viral RNA by blocking degradation from cellular exonucleases, protecting the viral RNA from destruction. The flavivirus 5' end is processed by RNA triphosphatase NS3 and then capped by guanylyltransferase activity of the NS5 and also methylated at the 2'O and N7 positions by the methyltransferase function that is also encoded in

NS5 (35). The cap structure is also an element that can be recognized by the host RNA decay pathway. The presence of a 5' cap and positional methylation on the cap may determine whether the viral RNA is considered defective or non-self and degraded (or not) by the RNA decay pathway (36). Immediately downstream of the cap structure are two highly conserved secondary RNA structures known as stem-loop A (SLA) and stem-loop B (SLB). These two non-coding RNA structure are variable in nucleic acid sequence across different flaviviruses and are important for genome cyclization, viral RNA synthesis, and translation (37) .

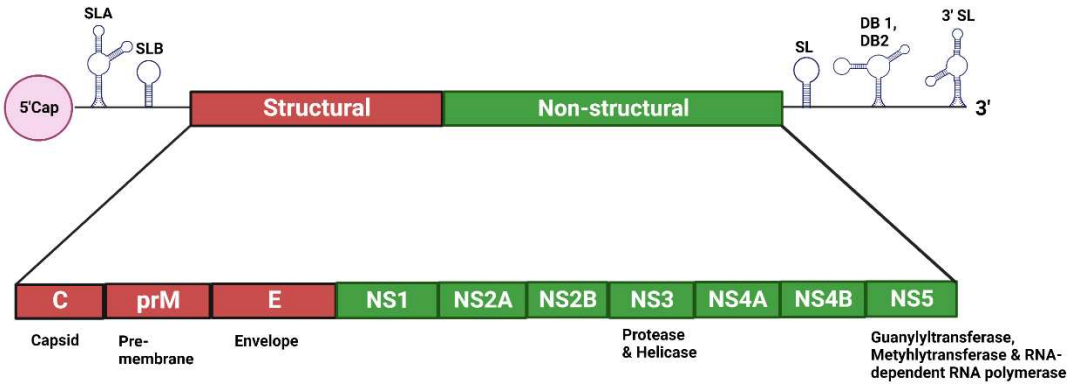

Fig. 2 ***The structure of the general flavivirus genome.*** Flavivirus genome typically contains non-coding regions (5' UTR and 3' UTR) and coding regions (structural and non-structural protein). Non-coding regions of flavivirus are highly structured that is important for genome replication and viral stability. The coding regions encode proteins needed to build physical structure of the virus and proteins necessary for viral genome replication (NS3 and NS5). Image generated by BioRender.

3.2 Flavivirus structural and non-structural proteins

Flavivirus genome encodes a single polyprotein that is co-translationally processed into mature proteins that can be grouped into non-structural or structural proteins. The structural proteins are responsible for building the physical architecture of the virus particle such as viral capsid (C), precursor membrane (prM), and envelope protein (E). The non-structural proteins are

essential for synthesizing the viral genome, and include NS1, NS2A, NS2B, NS3, NS4A, 2K, NS4B, and NS5. The NS1 protein is known to assist the formation of replication complex in the endoplasmic reticulum (ER) and the deletion of NS1 has been demonstrated to prevent infection and replication (38). Furthermore, NS1 is also an important protein marker for acute infection and interacts with complement immune response (39,40). NS2A protein plays a role in the assembly of virions by recruiting RNA from the replication complex into the packaging site (41). Conversely, NS2B is a cofactor of NS3 protein to stabilize the heterodimeric formation of NS3 ensuring the proteolytic activity of NS3 functions properly (42). NS3 possesses two domains, the N-terminal protease domain which aids in the maturation of viral proteins by cleaving the polyprotein produced during viral translation into fully functional proteins. The C-terminal domain functions as an RNA helicase that unwinds double-stranded RNA during the replication process. NS4A plays multiple roles in viral replication such as membrane remodeling, an antagonist of interferon pathways, and involved in the formation of viral replication complex (along with NS4B) (43). Lastly, NS5 serves as RNA-dependent RNA polymerase (RdRP) essential for the replication of viral negative and positive strand RNAs. Due to the flavivirus genome conformation being a single-stranded positive-sense RNA, the virus encodes its own RNA dependent RNA polymerase. Additionally, NS5 is also responsible for capping viral RNA through a two-step reaction. The N-terminal methyltransferase/guanylyltransferase domain of NS5 utilizes GTP and converts it into a GMP-enzyme intermediate. The GMP-intermediate is subsequently transferred to the diphosphate end of RNA transcript generated by the NS3 RNA triphosphatase activity to form the unmethylated GpppN structure (44). Finally, the guanosine in the cap is methylated by guanine-N7 methyltransferase that is also encoded in the N-terminal of

NS5 to form cap 0, and the 2' hydroxyl on the ribose moiety of the first viral base is methylated to form cap 1 (45).

3.3 Flavivirus 3' UTR structure and its significance

The 3'UTR region of the flavivirus genome contains stem-loop pseudoknot structures critical for viral genome replication and protection (Fig 2). The three helix junction / pseudoknot structures, called xrRNAs, interact with the host RNA decay pathway and produces subgenomic flavivirus RNAs (sfRNA) (46). The sfRNAs suppress the cellular RNA decay process by inhibiting the host enzyme XRN1, which is accomplished by the XRN1 enzyme becoming "stuck" on the RNA and not being able to completely degrade the viral RNA, which results in the sequestration of XRN1. Sequestration of XRN1 is thought to protect other viral genomes from degradation, and also results in dysregulation of cellular gene expression and antiviral responses (47,48). Therefore, sfRNA production is beneficial to the virus in stopping the RNA decay process and prolonging viral replication (47). Additionally, sfRNA generation also play a major role in determining disease outcome and successful replication. A study using mice and WNV as a model showed that mutant virus that lacking xrRNA structures did not form sfRNAs and failed to replicate in wildtype mice (48).

4. The cellular RNA decay pathway and its potential antiviral nature against viral RNA

The key to a successful flavivirus replication lies in their ability to deliver and keep their RNA genome intact in the host cytoplasm. However, once they get inside the cytoplasm, viral RNA gets scrutinized by cellular RNA quality control and processes. One pathway that interferes

with viral RNA and holds the potential to control and degrade viral RNA is known as the RNA decay pathway. There are multiple RNA decay pathways exist such as 5'-3'decay, 3'-5' decay, nonsense-mediated decay, and no-go decay. In this study, we will be focusing on 5'-3' exonucleolytic decay and their interaction with flaviviruses replication. RNA decay pathway is an important quality control system that oversees the proper gene expression within our cells (49). The RNA decay pathway is partially responsible for regulating the amount of RNA that is available for translation (50). The connection between the major RNA decay pathway and protein translation lies in the fact that efficient protein synthesis needs destabilization of closed loop mRNA structure. Therefore, increased translation initiation happened when mRNA degradation is inhibited and vice versa (50). The RNA decay pathway also works by scanning the irregularity in the structure and sequence within the RNA. Upon finding the target RNA, RNA decay factors and RNA decay enzymes starts to break down the RNA through several steps (51). Normal cellular mRNAs undergo co-transcriptional modification such as the addition of a 5' methylated cap and poly-A sequences at the 3' terminus to become fully mature and active. These modifications not only increase the stability of the RNA by blocking exonuclease access but also helps differentiate between self RNAs from foreign RNAs, such as viral RNAs. The lack of these molecular markers and stabilizing elements on an RNA in the cell will potentially initiate a series of molecular events that result in the degradation of the offending RNA. Additionally, RNA with nonsense sequences, such as premature termination codons in their sequence, can be detected and degraded by the RNA decay pathway (52).

The RNA decay pathway is divided into the exonucleolytic pathway (deadenylation dependent and independent) and the endonucleolytic pathway (51). The exonucleolytic pathway

can be initiated by the deadenylation process where the poly-A tail sequence will be degraded by CCR4-NOT or PARN. Once the poly-A tail is cleaved, an exosome complex consisting of Lsm1-7 proteins recruits decapping enzymes such as DXO, DCP1, and DCP2 (5'-3' decay pathway). These decapping enzymes cleave the 5' cap and remove the guanosine and two phosphates (gamma and beta phosphate) leaving a single 5' monophosphorylated RNA as the product. The single monophosphorylated RNA can then serve as a substrate for RNA degradation by exonuclease XRN1. Alternatively, monophosphorylated RNAs can also be formed from non-capped triphosphorylated RNA (ppp-RNA) through the function of RNA triphosphatases such as DUSP11 and NUDT2. DUSP11 and NUDT2 have been shown to remove the diphosphate group from ppp-RNA to form monophosphorylated RNAs (53,54)(Fig. 3). The role of RNA triphosphatases in the RNA decay pathway is not fully laid out yet, and further studies are needed to elucidate the complete role of these proteins in the RNA decay pathway. Additionally, 3'-5' decay can also happen by the recruitment of exosomes that degrades the RNA from the 3' end. During the 3'-5' decay process, the RNA decapping process is carried out by the scavenger decapping enzyme, DcpS. Both the 5'-3' and 3'-5' decay pathways require deadenylation of cellular mRNA, a process known as deadenylation-dependent mRNA decay. Exonucleolytic-mediated RNA decay pathway can also be initiated without the deadenylation step. The deadenylation-independent RNA decay pathway is found mostly in yeast but it is not clear whether it operates in mammalian cells (55). Once the RNA is decapped, XRN1 initiates 5'-3' decay from the 5' end of the RNA. The endonucleolytic pathway is characterized by endonuclease cleavage within the RNA. Some examples of endonucleases involved in the process are IRE1, PMR1, G3BP, MCPIP, SMG6, APE1, and RNase MRP (56–62). These

enzymes cut the RNA into two fragments that can be further degraded by exosomes or XRN1 mediated decay.

Generally, viral RNAs are different than cellular mRNAs. These differences can be sensed by our RNA decay pathway and hypothetically processed for degradation. Flavivirus genomes contains a 5' N7/2'O methylated cap (cap 1) with a 3' highly structured stem-loop known as xrRNA (63) and do not contain a poly(A) tail. The 3' UTR stem-loop structure in flavivirus RNA has implications on our cellular RNA decay pathway. During infection, RNA decay pathway will initiate flavivirus RNA degradation in cytoplasm. In cytoplasm, flavivirus RNA may undergo decapping by decapping enzymes such as DXO, DCP1, and DCP2. Monophosphorylated RNA formed after decapping process will then undergo degradation by XRN1. However, due to the highly structured 3'UTR of flaviviruses, incomplete degradation and stalling of XRN1 occurs. This resulted in the formation of subgenomic flavivirus RNAs (sfRNA) (46). Although it is very clear that XRN1 plays a major role in the formation of sfRNA, it is unclear how the monophosphorylated viral RNA substrate for XRN1 is generated. Presumably, monophosphorylated RNA can be formed as the product of cellular decapping enzymes or generated by RNA triphosphatase enzymes. Data obtained from a collaboration between the Geiss and Wilusz laboratories showed that the flavivirus genomes isolated from viral particles may contain a significant fraction of uncapped viral RNA genomes (Fig. 3). These uncapped genomes may represent a class of viral RNA molecules that are delivered to cells via infection and if they come in triphosphorylated form, they may provide substrates for XRN1 degradation and subsequent inhibition early in infection. The origin of these uncapped flavivirus RNA has not been previously defined, and ***the goal of this project is to clarify how these uncapped viral***

RNAs are generated during infection. Characterizing how these uncapped viral RNAs are generated can improve our understanding of how flaviviruses actively evade the RNA decay pathway and subvert cellular processes during infection.

The presence of uncapped flavivirus RNA is intriguing, but the structure of the uncapped RNAs present during the infection is currently unclear. The experiment in Figure 3 was performed by RNA cap immunoprecipitation and quantification of input, precipitated, and unprecipitated fractions, but it was not determined what the 5' phosphate end structure of these uncapped RNAs actually was. These RNAs could come in three different 5' phosphate conformations, triphosphorylated, diphosphorylated, and monophosporylated. If the majority of the uncapped RNA population is triphosphorylated, triphosphatase enzymes such as NUDT2 and DUSP11 can convert the RNA into monophosphorylated RNA form that can be degraded by XRN1. NUDT2 can also convert diphosphate RNAs to monophosphates. RNA decapping enzymes such as DXO and DCP2 can remove previously formed caps to generate monophosphorylated RNAs that are degradable by XRN1. One of these gene products may be responsible for forming the uncapped RNA fraction found in virions, but this has not been studied until this project.

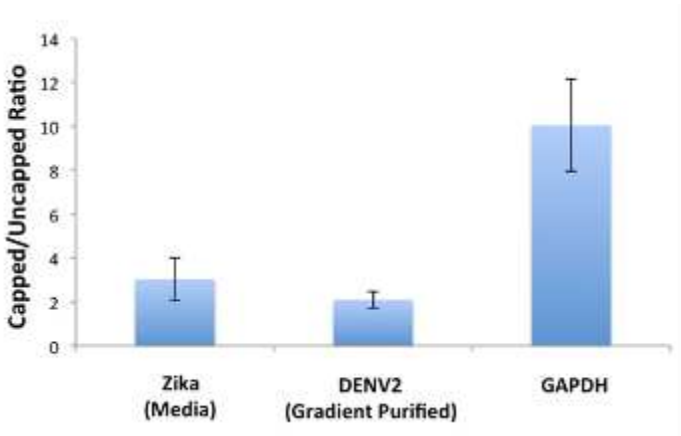

Fig. 3 ***Capping ratio of different flavivirus.*** Immunoprecipitation specific to m7G capped antibodies were performed in cells infected with ZIKV or DENV2. The data showed that there are approximately 25% uncapped RNA in ZIKV infected samples and 33% in DENV2 infected samples.

4.1 Interactions between viral RNA and cellular RNA decay pathway

The constant stress from the cellular RNA decay pathway to degrade viral RNA creates an evolutionary pressure for viruses to develop strategies to evade decay. In flaviviruses, namely ZIKV, the viral evasion mechanism includes the production of interfering structural protein such as capsid that can bind to and cause the destruction of RNA decay factors such as Upf1 (64). In WNV and Hepatitis C Virus (HCV), viral capsids have also been shown to inhibit the nonsense-mediated RNA decay pathway by interfering with the formation of RNA decay complex (65). Additionally, some flavivirus also enhance their RNA stability by synthesizing their own 5' cap and adding xrRNA stem-loop structures to stall and divert the cellular RNA decay process (XRN1) (66). Understanding more about how the cellular RNA decay pathway is inhibited by viral proteins and processes will uncover the way to restore RNA decay pathway function and possibly help in providing means to stop the virus.

5. RNA decay proteins studied in this project and their roles in the RNA decay pathway

XRN1 is a highly conserved and processive exonuclease that degrades monophosphorylated RNA from 5' to 3' direction (Fig. 4). For XRN1 to be able to initiate degradation, the substrate RNA needs to be decapped and reduced to a monophosphorylated RNA (67). Several decapping enzymes such as DXO, DCP1, DCP2, and NUDT16 have been known to catalyze decapping process and forming monophosphorylated RNA (68). Uncapped RNA requires different enzymatic process, instead of decapping enzymes, triphosphatase enzymes can digest triphosphorylated RNA into monophosphorylated RNA. To date DUSP11 and NUDT2 have been identified to be able to form monophosphorylated RNA from uncapped triphosphorylated RNA (53,69) . XRN1 dysregulation has been linked with several pathophysiological conditions such as cancer, neurodegenerative disease, diabetes, and obesity (70–72) .

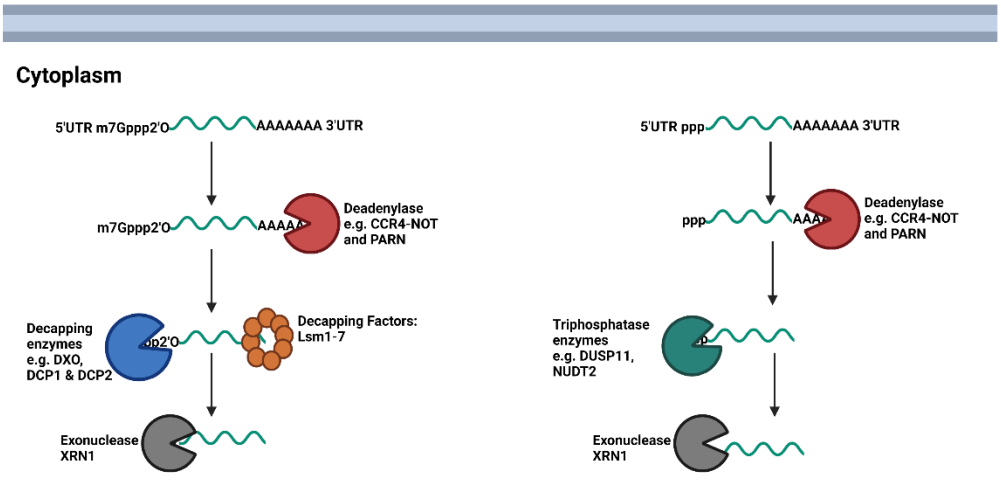

Fig. 4 ***Cellular RNA decay pathway between RNA with a 5' cap and without the cap.*** Proposed model of deadenylation dependent 5'-3' exonucleolytic decay, depending on the capping status of the RNA substrate, different enzymes are needed to process and reduce the RNA into a monophosphorylated form that can be digested by exonuclease XRN1. Image generated by BioRender.

DXO is a decapping enzyme that acts on defective mRNA transcripts. DXO recognizes incomplete unmethylated 5' caps on mRNAs, removes the cap, and the decapped RNA undergoes 5'-3' exonucleolytic decay by DXO (73). Interestingly, since DXO decapping activity is blocked by the presence of 2'O methylation on the m7G cap, this suggests that DXO activity may be specific in degrading non-self-RNA (73). Other than its decapping and exonucleolytic activity, DXO also possesses other enzymatic activities such as deNADing and pyrophosphohydrolase (74,75). Due to its substrate preference for unmethylated mRNA, DXO is vital in the quality control of pre-mRNA capping (76). Furthermore, DXO has been suggested to be a restriction factor for flaviviruses and alphaviruses (77). Consequently, studying the role of DXO during viral infection may reveal a novel strategy to inhibit viral replication.

DCP2 regulates mRNA levels by removing the 5' cap structure of mRNA and leaving a monophosphorylated RNA. It activates the decapping process by interacting with activator proteins such as Dcp1, Edc1, and Edc3. The decapping activity of DCP2 lies on its Nudix hydrolase motif, and DCP2 has been shown to remove caps from m7G caps whether it is methylated at the 2'O or not (78), a key difference with DXO. A genome-wide RNAi screening showed that loss of DCP2 increased Rift Valley Fever Virus (RVFV) (bunyavirus) replication without affecting mRNA stability, proving that DCP2 is antiviral factor for RFVF (79). Additionally, DCP2 activity can modulate the RNA level of IRF-7, which is essential for the interferon response (80). Both these studies hinted that DCP2 may play a role in suppressing viral infection. However, studies regarding DCP2's role in positive strand virus infection are very limited. Therefore, more studies on DCP2 during viral infection may unlock information on how DCP2 interacts with the RNA viruses and viral RNA genomes.

DUSP11 is an RNA triphosphatase enzyme that cleaves gamma and beta phosphate from 5'-triphosphorylated RNA resulting in 5'-monophosphorylated RNA (81). 5'-monophosphorylated RNA is a substrate recognized by XRN1 exonuclease that promotes RNA degradation. Through this mechanism, DUSP11 plays a role in the regulation of innate immunity through the RIG-I receptor activation. DUSP11 works by decreasing the presence of cellular 5'-triphosphorylated RNA, the known ligand for RIG-I activation. Consequently, a reduction in 5'-triphosphorylated RNA will decrease RIG-I activation and fine-tune the interferon response (antiviral response) (82). On the other hand, the lack of DUSP11 activity can potentially resulted in the abundance of 5'-triphosphorylated RNA that will induce RIG-1 activation and may cause autoimmunity (83). Therefore, DUSP11 is important in maintaining the triphosphorylated RNA balance inside the cells and ensuring a proper innate immune response. During infection, the presence of DUSP11 can be beneficial or detrimental to the virus. It can be beneficial by reducing the interferon response needed to clear the infection. For example, in Vesicular Stomatitis Virus (VSV) infection, DUSP11 proved to be proviral as it helps to dampen the activation of RIG-I receptors (84), i.e. decreasing viral RNA visibility to the RIG-I receptor. In some viruses, such as Hepatitis C virus (HCV), DUSP11 activity is antiviral to the virus. DUSP11 helps process the HCV ppp-RNA into the p-RNA form that is susceptible to XRN1 mediated degradation (54). Additionally, the reduction of DUSP11 is associated with lytic reactivation of Kaposi Sarcoma Herpes Virus (KSHV) in infected cells (85). The proviral or antiviral effect of DUSP11 may depend on the capability of the virus to salvage or hijack DUSP11 functions for its replication. Therefore, further studies are needed to define the

interaction between different viruses and DUSP11 as their interaction need to be addressed on a case-by-case basis.

NUDT2 is another RNA triphosphatase enzyme that cleaves gamma and beta phosphates from triphosphorylated RNA to generate monophosphorylated RNA. NUDT2 shares homology to bacterial RNA pyrophosphohydrolase H (RppH) that works against di- and triphosphorylated RNA. Unlike DUSP11, NUDT2 has also been shown to possess decapping activity and generate diphosphorylated and monophosphorylated RNA (86). In an *in vitro* study with vesicular stomatitis virus, NUDT2 showed antiviral capacity and the depletion of NUDT2 increased viral growth (53). Although there is an indication that NUDT2 can limit infection, more studies are needed to fully elucidate the role of NUDT2 in virus infection, especially in flaviviruses.

The study of RNA decay pathway component interaction with viral RNA during infection is still very limited. Based on the current literature, we can conclude that the RNA decay pathway interacts differently with different viruses. Some viruses are inhibited by RNA decay pathway activity, some others develop evasion mechanisms and can hijack the pathway for their own gain. Therefore, extensively studying the effect of the RNA decay pathway in different RNA viruses, such as flaviviruses (the focus of this project) can be beneficial in uncovering novel approaches that target viral replication. In this study, we aim to understand the role of four key enzymes in cellular RNA decay pathways DUSP11, DXO, NUDT2, and DCP2 (Fig.5). We performed loss of function experiments by knocking down the RNA for each these proteins in human Huh7 cells using RNA interference (RNAi). We hypothesized that DUSP11 and NUDT2 due to their triphosphatase activity may help increase the visibility of uncapped viral RNA to

exonucleolytic degradation by XRN1 if the uncapped viral RNAs are tri- or diphosphorylated. Alternatively, we also hypothesized that DXO and DCP2 activity may be involved in processing of capped viral RNA to uncapped monophosphorylated forms for RNA decay. Knocking down genes could result in inhibition of viral RNA degradation and thus cause an increase production of the virus, therefore demonstrating that DUSP11, NUDT2, DXO, and/or DCP2 are antiviral effectors against flavivirus RNAs. However, flaviviruses are known for their ability to stall XRN1 due to their xrRNA pseudoknot structures and generation of sfRNAs which can repress cellular antiviral responses, so DUSP11, NUDT2, DXO, or DCP2 knockdown could prove inhibitory to viral replication (Fig. 4). Therefore, the experiments that we propose will help define how these critical RNA decay genes influence flavivirus infection in human cells.

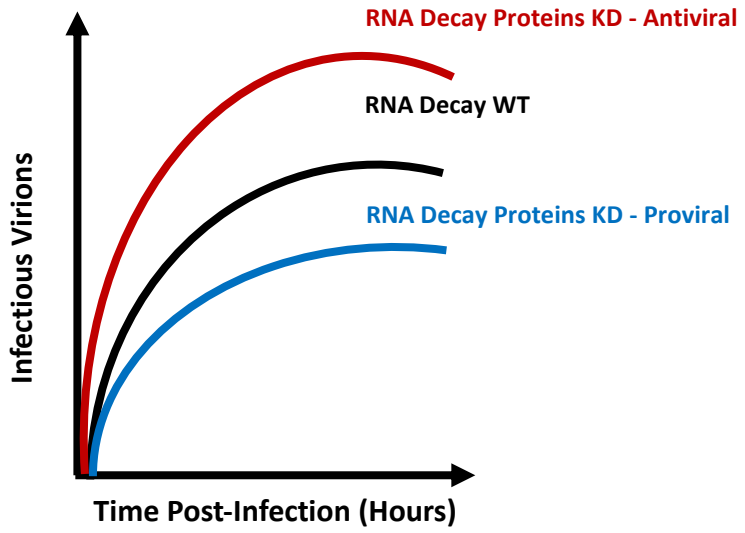

Fig. 5 ***Different outcomes of the loss of RNA decay pathway proteins.*** A schematic diagram that showed different effects of siRNA-mediated knockdown impact on flavivirus replication. If the RNA decay protein is antiviral, higher production of infectious virus will be observed in the absence of RNA decay protein. On the other hand, if the RNA decay protein showed proviral effect, lower titer of virus production will be observed.

We screened the effect of different RNA decay proteins knockdown in two different systems. We first used a luciferase replicon (plasmid-based) system to help quantify the viral

RNA production in the knocked down cells. Our initial data from the replicon assay showed that triphosphatases (DUSP11 and NUDT2) knockdown enhanced the production of viral RNAs, and depletion of DCP2 dampens the production of replicons. We then performed infectious virus assays (at 24 and 48 hours) using authentic West Nile virus, Zika virus, and Yellow Fever 17D viruses in Huh7 cells depleted of DUSP11/DXO/NUDT2/DCP2. We collected supernatants from infected cells to measure the production of infectious viruses and viral RNA. We also gathered cellular pellets to verify the efficiency of RNA knockdown and quantify intracellular viral RNA production. Our authentic flaviviruses infection showed that DUSP11 and NUDT2 knockdown did not affect the infectious virus and viral RNA production, contrasting our initial replicon assay findings. Intriguingly, reduction of DCP2 in Huh7 cells consistently resulted in lower infectious virus and viral RNA production. These data suggest that DCP2 may play a role in manufacturing infectious flaviviruses and DCP2 acts as a proviral factor during infection. Overall, our data showed that DCP2 is important to the replication of flaviviruses, a novel finding in the flavivirus field.

MATERIALS AND METHODS

Cell Lines and Viruses. Human Huh7 (hepatocarcinoma) cells were obtained from Dr. Rushika Perera, CSU. African green monkey Vero (CCL-81) cells were obtained from ATCC. All cells were grown using DMEM (Gibco) supplemented with 1% Penicillin-Streptomycin (Cytiva), 1% L-glutamine (Gibco), 12.5 mM HEPES (Life Tech), and 10% Fetal Bovine Serum (FBS). Cells were incubated at 37^{o}C with 5% CO_2. Flaviviruses used in this study were a Lineage II West Nile virus engineered to express GFP (87), Zika virus (strain PRVABC59) (88), and yellow fever virus (strain 17D) (89). Viruses' stocks were all grown in Vero cells using DMEM supplemented with 2% FBS and 50 mM HEPES (pH 7.5). Viral titers were obtained with focus forming assay (described below) and described as FFU/ml.

Plasmids. West Nile virus replicon expression plasmids (pBG438, pBG508) were used in the replicon assay (87,90). pBG438 contained the 5' and 3' UTR regions, associated RNA structures within the capsid open reading frame, as well as the nonstructural NS1, NS2a, NS2b NS3, NS4a, 2K, NS4b, and NS5 open reading frame from Lineage II West Nile virus. Firefly luciferase was fused to the capsid protein, and a FMVD-2A translational skip site is present between the luciferase gene and a residual envelope ER transmembrane signal sequence to provide convenient reporting on viral translation. A selection marker blasticidin deaminase was present in the replicon RNA but was not used for these experiments. As a non-replicating control, a NS5 RNA dependent RNA polymerase GVD mutation that inactivates polymerase activity was engineered to make plasmid pBG508. The complete structure of the replicon expression cassette and resultant replicon can be seen in Figure 6. Upon transfection, pBG438 or pBG508 will be deposited in the nucleus and viral replicon RNA transcribed from a cytomegalovirus IE promoter by Pol II in the nucleus. To obtain

accurate viral RNA 3' end sequences, the sequence for a Hepatitis delta virus ribozyme (HDVr) was added to the end of the replicon genome. The ribozyme will cleave away the ribozyme and downstream 3' UTR and poly-A tail sequences from the replicon RNA, leaving an authentic 3' viral RNA end. Replicon replication is monitored in transfected cells using firefly luciferase activity as described below.

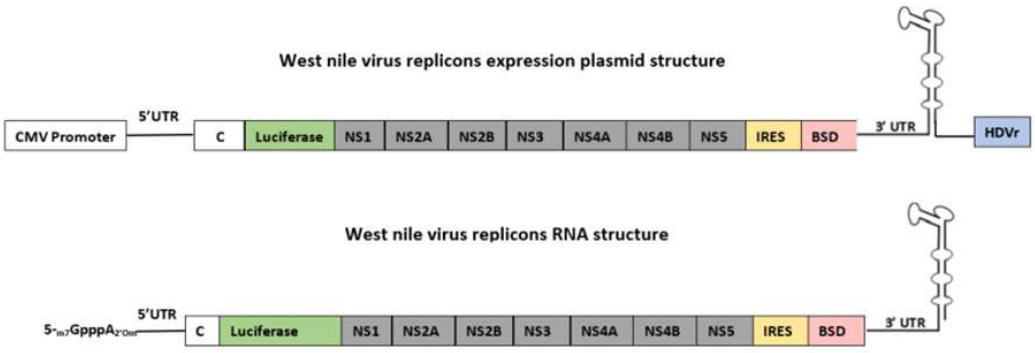

Fig. 6 ***Complete structure of pBG 438.*** Replicon was constructed according to WNV lineage II non-structural proteins. Structural proteins such as pre-membrane and envelope were removed, although small portion of viral capsid sequence was used to initiate translation. Luciferase gene was inserted to help quantify the production of the replicon.

Immunoblots. Transfected or infected cells were trypsinized, centrifuged, and resuspended in 20µl PBS. Resuspended cells were boiled for 5 min in Laemmli Buffer (Bio-Rad) with Beta-mercaptoethanol as the reducing agent. Equal volumes of cell lysate were then loaded onto 15% acrylamide gels, resolved by electrophoresis, and then transferred onto PVDF (Sigma Aldrich) membrane. Transferred membranes were blocked with a 1x TBS-T (20 mM Tris, 150 mM sodium chloride, 0.1% Tween-20) - 4% skim milk blocking solution. After incubation, membranes were washed with 1x TBS-T and primary antibodies (rabbit polyclonal) were added at the dilutions listed in Table 1 and incubated at 4^{o}C overnight. After overnight incubation, membranes were washed 5 times with 1x TBS-T. Secondary antibodies (goat anti-rabbit (Abcam)) were added at

1:10,000 dilution, incubated for 1 hours at room temperature, and membranes were washed 5X with TBS-T. Protein bands were visualized using Pierce TMB Substrate Kit (Thermo Fisher) and then captured with digital camera or scanner.

Table 1 List of primary and secondary antibodies used for western blots

Primary Antibodies (Goat anti Rabbit Polyclonal Antibodies)	**Brand**	**Cat#**	**Dilution**
GAPDH	Novus-biologicals	NB100-56875	1:2000
DUSP11	Protein Tech	10204-2-AP	1:1000
DXO	Novus-biologicals	NBP1-56979	1:1500
DCP2	Novus-biologicals	NBP1-41070	1:2000
NUDT2	Protein Tech	10484-1-AP	1:4000

siRNA mediated knockdown assay. To analyze the effects of different RNA decay proteins against virus infectivity, siRNAs targeting RNA decay pathway genes were used (Table 2). Nonspecific siRNA was used as negative control and gene of interest siRNA (DUSP11, DXO, NUDT2, and DCP2) were obtained from Ambion. Huh7 cells were harvested and plated in 6-well plates at 30,000 cells/well with DMEM supplemented with 10% FBS. Following an overnight incubation 37^{o}C; 5% CO_2, cells were transfected with a 1 µm siRNA and 2.4 µl lipofectamine RNAiMAX transfection reagent according to the manufacturer's protocol. Cells were then incubated at 37^{o}C; 5% CO_2 for 48 hours.

Cell Viability Assay. To assess the effect of siRNA knockdown in Huh7 cells, cells were plated in 96-well plate with the density of 1.000 cells/well. Following overnight incubation at 37^{o}C in 5% CO_2, Huh7 cells were then transfected with siRNA as described in the previous paragraph and

incubated for 48 hours. Viability test was performed using CellTiter-Glo kit (Promega) according to the manufacturer's protocol. Luminescence reading was analyzed using Prism Graphpad.

Table 2 List of siRNAs used to knockdown RNA decay proteins

Target	**Cat. No or Assay ID (according to Ambion website)**
Negative Control	4390843
DUSP11	s16030
DXO	s4240
DCP2	128049
NUDT2	s194286

WNV Replicon Assays. Huh7 cells were harvested and plated at 1,000 cells/well in 96-well using DMEM supplemented with 10% FBS. After 24 hours, cells were transfected with siRNA and Lipofectamine RNAiMAX according to the manufacturer's protocol. Cells were then incubated at 37^{o}C in 5% CO_2 for 48 hours. After incubation, cells were transfected with replicon expression plasmids pBG438 (wildtype) or pBG508 (replication defective) using Lipofectamine 2000 according to the manufacturer's transfection protocol. After the addition of replicons, cells were incubated at 37^{o}C 5% CO_2 for an additional 48 hours, then measured for cell viability and firefly luciferase activity using One Glo and Tox Luciferase reporter and cell viability assay (Promega) following the manufacturers recommendations. Data was analyzed in Prism Graphpad.

Infection assay of siRNA knockdown cells. Viruses used in this project were West Nile lineage II virus (WNV) (Accession number: NC_001563), Zika virus (ZIKV) (Accession number: KU501215), and yellow fever 17D virus (YFV) (Accession number: NC_002031). After 48 hours of siRNA mediated knockdown assay, Huh7 cells were infected with indicated virus with multiplicity of infection (MOI) of 0.01. Following initial infection, cells and supernatants were

harvested at 24- and 48-hours post-infection. Cell supernatants were aliquoted and used for viral quantification with reverse-transcriptase digital droplet PCR (RT-ddPCR) (Bio-Rad) and infectivity assays using Focus Forming assay. Cell lysates were divided into two aliquots, the first aliquot for western blot analysis (lysed with Laemmli buffer) and the other aliquot treated with Trizol reagent (Thermo scientific) for RNA extraction using Direct-zol RNA Mini-prep kit (Zymo Research) and subsequent RT-ddPCR analysis.

Focus Forming Assays. Vero cells were seeded into 24 well plate to achieve confluence the next day. Virus samples were prepared in dilutions from 10^{-1} to 10^{-6} in infection medium. Growth medium in 24 well plates was aspirated, and virus samples were transferred to each designated well. Infected samples were incubated for 1 hour in 37ºC in 5% CO_2 before the addition of 1% agarose/DMEM overlay medium. Plates were then incubated for several days depending on the virus samples (4 days for WNV and YFV, 3 days for ZIKV). After the incubation finished, 10% formaldehyde was added to each well to fix the cells. After 30 minutes, formaldehyde and agarose plugs were removed, and wells were washed with PBS three times. After formaldehyde fixation and PBS washes, cells were incubated with perm wash buffer (1% BSA and 0.3% Tween 20 in PBS) for 15 minutes. Perm wash buffer were then removed and primary antibody 4G2 was added. Plates were then incubated at 4ºC overnight. 4G2 flavivirus envelope primary antibody used in this experiment was generated from hybridoma cells obtained from ATCC (D1-4G2-4-15). The next day, wells were washed with TBS-T three times and secondary antibody (goat anti mouse IgG-HRP) were added to each well. Plates were then incubated for two hours and then washed with TBS-T to remove residual antibody. To visualize the immunospots, the Pierce TMB Substrate Kit solution (Thermo Fisher) was added to each well and incubated for 10 minutes. Immunospots were counted and used to calculate FFU/ml values. Data was analyzed in Prism Graphpad.

Viral quantification and gene quantification. Viral genome quantification was performed using primers that target viral positive strand RNAs in the polyprotein open reading frame (Table 1). Viral RNAs were extracted from infected supernatants using the QIAamp Viral RNA kit (Qiagen), and Total RNAs were extracted from cell lysates using Direct-Zol RNA Mini-prep kit (Zymo research). Eluate from the direct-zol extraction process were assessed for RNA concentration and purity using Nanodrop and then normalized to achieve 50 ng of RNA. Viral cDNA was then synthesized using Improm-II Reverse Transcriptase enzyme (Promega). BG1808 was used as the reverse primer to generate the WNV cDNA. For ZIKV and YFV cDNA generation, BG1119 and BG1382 were used for reverse transcription. For viral quantifications, ddPCR was performed using viral cDNA from supernatant and total RNA samples using a BioRad ddPCR system. RNA samples were diluted up to 1000x to produce clear droplets separation. Master mix for ddPCR was prepared as per manufacturer's protocol for Evagreen ddPCR supermix (Bio-Rad). Droplet generation was performed using a Bio-Rad QX100 droplet generator. Dropletized master mixes were then thermocycled for 40 cycles according to Evagreen ddPCR mastermix manufacturer's protocol. Once thermocycling was finished, plates were read with a Bio-Rad QX200 droplet reader. For gene quantification, total cDNA from cell lysates were diluted to achieve 1 ng for GAPDH and 10 ng for gene of interest (DUSP11, DXO, NUDT2, and DCP2). A detailed list of primers used can be seen in Table 1. Positive droplets were counted and calculated to obtain gene copy number/ml value.

Table 3 List of primers used for viral quantification and gene quantification:

Name	Target	Primer sequence (5'-3')
BG1808	WNV NS5 reverse primer	TGGTGTCTTCATACCTCCTCAAGG
BG1809	WNV NS5 ddPCR reverse primer	TGCCACACCAAATGTCCTCTCT
BG1810	WNV NS5 ddPCR forward primer	CTGGAACAGAGTGTGGATTGAGGAG

BG1118	ZIKV NS1-NS2A forward primer	ATAAGGCCCAGGAAAGAACC
BG1119	ZIKV NS1-NS2A reverse primer	AGCAGGATCACAAGCACTCC
BG1381	YF NS5 forward primer	GCACGGATGTAACAGACTGAAGA
BG1382	YF NS5 reverse primer	CCAGGCCGAACCTGTCAT
BG743	GAPDH – huh7 – forward	CTCTGCTCCTCCTGTTCGAC
BG744	GAPDH – huh7 – reverse	TTAAAAGCAGCCCTGGTGAC
BG1812	DUSP11 - human – forward	TGGTGTCCACTGTACCCATGG
BG1813	DUSP11 - human – reverse	TTCTAAGCAATGTCCCCGGCA
BG1814	DXO - human – forward	TGACGACACCGTATGAGCGG
BG1815	DXO - human – reverse	ACATAAGCTCCCGGAGGAGC
BG1816	DCP2 - human – forward	TCCGCCACAGTCAGCAGTTAT
BG1817	DCP2- human – reverse	TCTTCACTGGAGCTAGGCAAGTC
BG1818	NUDT2 - human – forward	CACTGGACTCCTCCCAAAGG
BG1819	NUDT2 - human – reverse	TCCTCTTGGGTCTCCCTCAG

***In vitro* XRN1 sensitivity assay.** An in vitro assay to examine flavivirus 5' phosphate status and sensitivity to RNA decay and to quantify proportions of monophosphorylated RNAs present in viral RNA samples was developed using in vitro transcribed RNAs as test targets, a recombinant commercial RNA decapping enzyme, and recombinant Xrn1 protein. In vitro RNA transcripts were generated from plasmids pBG742 that encode 5' UTR but lacks Stem-loop A structure of WNV lineage II and pBG741 that contains SLA in the WNV Lineage II 5'UTR. To generate RNA transcripts, pBG741 and 742 were both linearized with EcoRI (New England Biolabs) and purified using a Zymo DNA purification spin column. Linearized plasmids were used in RNA transcription reactions using the MEGAshort script T7 (Thermo Fisher) kit with modified nucleotide composition to generate di- and monophosphorylated RNAs. To produce monophosphorylated RNA and dephosphorylated RNA, AMP and ADP were added in 10-fold excess to ATP, respectively, to the in vitro transcription reactions. Triphosphorylated RNAs were generated using the standard nucleotide mixture without addition of extra nucleotides or analogs. To obtain capped

RNA, triphosphorylated RNA was used as the substrate with the addition of GTP and commercially available Vaccinia virus capping enzyme (New England Biolabs). RNAs were purified using phenol:chloroform extraction and quantified by both Qubit and urea gel electrophoresis with Sybr Gold. Two groups of RNAs were generated, the first group containing the WNV stem-loop A (SLA) structure in the 5' UTR (synthesized in four conformations: capped, triphosphorylated, diphosphorylated, and monophosphorylated RNA) to represent the native 5' end structure of WNV, and a second group lacking the SLA structure.

To assess RNA sensitivity to decapping and XRN1 degradation, 200 ng of each RNA was used in four separate enzymatic reactions: XRN1 and mRNA decapping enzyme (MDE, recombinant yeast DCP1/DCP2), XRN1 only, MDE only, and no enzyme. XRN1 and MDE enzymes were both purchased from New England Biolabs (NEB). For XRN1 only, MDE only, and no enzyme reactions, the reported storage buffer of enzymes that were not used in the experimental conditions were added to equilibrate buffer compositions across different enzymatic treatments. For example, the XRN1 only reaction would contain the addition of MDE storage buffer and MDE reaction buffer. For the MDE only reaction, XRN1 storage buffer and XRN1 reaction buffer were added. Lastly, for no enzyme, both enzymes storage and reaction buffer were added. Xrn1 sensitivity reactions were set up with RNA and MDE enzyme (or storage buffer) and Murine RNase inhibitor (New England Biolabs) first and incubated for an hour at 37^{o}C. XRN1 (or storage buffer) was then added, and the reaction was incubated for an additional hour at 37^{o}C. To stop the reaction, RNA was extracted using the RNA clean & concentrator (Zymo research) system. To visualize the degradation of RNA after the assay, RNAs were resolved on 15% Urea-polyacrylamide gel for 45 minutes at 200 volts, gels stained with SYBR-Gold (Invitrogen) for 30 minutes, and gels imaged using a GelDoc EZ-Imager (Bio-rad). Band intensity was analyzed using ImageJ software.

Statistical Analysis. Statistical analyses were performed using multiple comparison one-way ANOVA (Dunnett's test) or two-way ANOVA (Dunnett's test) with Graphpad Prism. Significant results were indicated when p-value <0.05.

RESULTS

1. NUDT2 knockdown affects Huh7 cells viability

To ensure that knockdown of RNA decay proteins did not significantly impact the viability of cells that were going to be used in this study, viability tests using CellTiter GLO were performed in Huh7 cells transfected with non-specific or RNA decay gene specific siRNAs. CellTiter GLO is a measurement of ATP that is present in metabolically active cells and therefore suitable to describe viability and the amount of metabolically active cells present post-transfection. Generally, knocking down (KD) RNA decay elements such as DUSP11, DXO, and DCP2 did not alter the viability of cells (Fig. 7). However, Huh7 cells that were deficient of NUDT2 protein showed a slight reduction in the number of viable cells remaining after 48 hours compared to control (Fig. 7). This reduction in viability, however, was not observed in the next part of experiment where we tested the viability of cells that were transfected with siRNA and replicons. In the future, viability factor was taken into calculation to normalize the data for our next experiments.

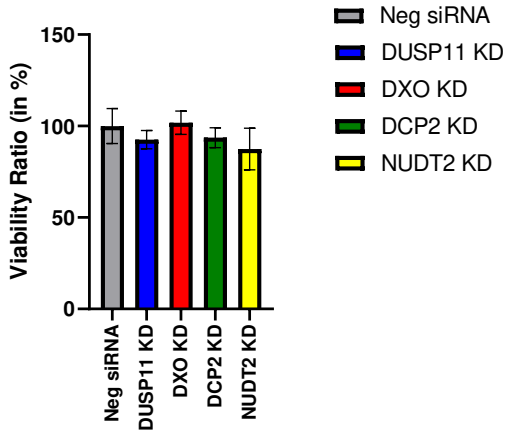

Fig. 7 ***siRNA knockdown of NUDT2 reduces cell viability of Huh7 cells but not for other RNA decay associated proteins*****.** Huh7 cells were transfected with different siRNA and after 48 hours post-transfection, medium was replaced, and viability was measured using CellTiter GLO. Luminescence reading were normalized and ratioed to control (Neg siRNA). Data points were obtained from two independent experiments and error bar represents standard deviation.

2. Knockdown of DUSP11, DCP2, and NUDT2 affect the production of replicons in Huh7 cells

To examine the effect of RNA decay proteins in flavivirus replication we initially used a WNV replicons that contain luciferase reporter gene to monitor viral replication. This simple system allowed us to quickly examine the effects of RNA decay proteins knockdown by measuring the luciferase expression as a readout for replicon replication. Cellular viability from siRNA and plasmid transfection is also factored in to equilibrate the luciferase readings of the samples. Based on the viability data, knocking down RNA decay proteins and transfecting the cells with the replicons slightly affected cell viability. Transfecting replicon alone and knocking down of DUSP11, DXO or NUDT2 did not significantly change viability of the cells compared to the control (Neg siRNA) (Fig. 8A). However, a slight reduction in the viability of DCP2 KD cells was observed (88% in DCP2 deficient cells vs 100% in Neg siRNA cells). Considering the decrease in cell viability, luciferase readings were normalized to viability ratio. Production of viral RNA using a replicon system is positively correlated with luciferase expression value, as luciferase protein expression is driven by viral protein translation. The more viral RNA formed due to genome replication, the higher the relative luciferase unit (RLU) is produced. Our data showed that knocking down the DUSP11 and NUDT2 RNA triphosphatases significantly increased the replication of viral RNA in the replicon system. This suggests that DUSP11 and NUDT2 may play a role in suppressing viral RNA production during infection. Interestingly, depletion of decapping enzymes such as DCP2 negatively affect the replication of flavivirus replicon. This indicates that the presence of DCP2 may be proviral and aid in the viral replication process. We did not see any significant changes in replicon production of DXO KD cells.

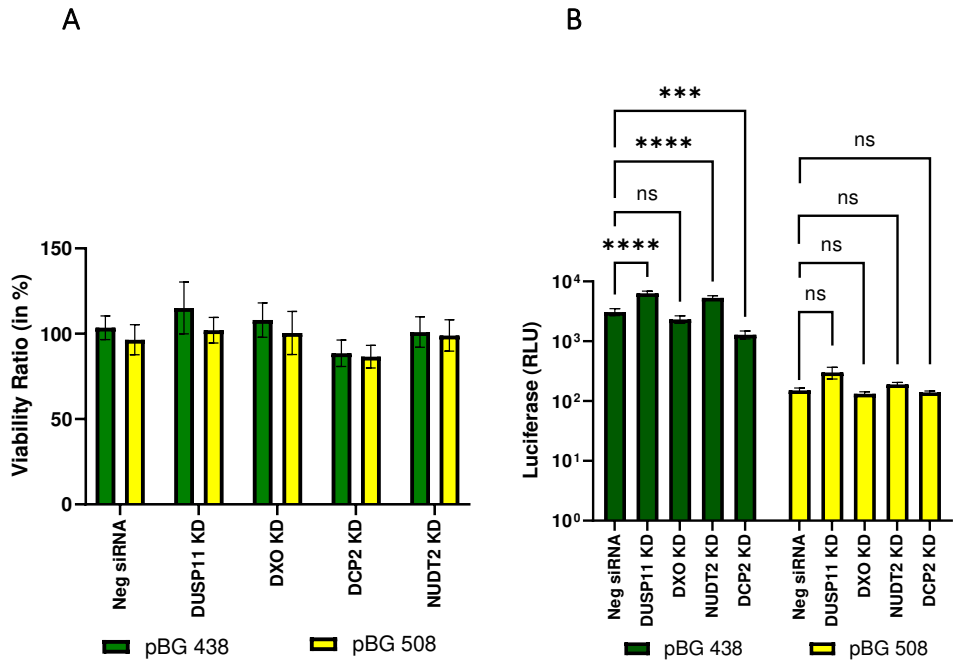

Fig. 8 ***Knockdown of RNA decay proteins marginally affect the viability and significantly alters the production of replicons in Huh7 cells.*** Huh7 cells were transfected with respective siRNA and then transfected with pBG 438 or pBG 508 as non-replicating control. After 48 hours, ONE-Glo + Tox Luciferase assay reagent were added to assess viability (A) and luciferase expression (B) of replicons. Fluorescence readings for viability test were normalized and ratioed to control (Neg siRNA). Viability ratios were used to equilibrate the luciferase expression readings. Data points were obtained from two independent experiments and error bar represents standard deviation. Asterisks represent statistical significance by two-way ANOVA (**** = p <0.001).

3. siRNA knockdown efficiency differs among different RNA decay proteins in WNV infected Huh7 cells

Confirmation of RNA decay protein knockdown was performed at the protein level using Western blot and at the RNA level using reverse transcriptase ddPCR. Huh7 cells were transfected with siRNA and then infected with West Nile virus were collected and proteins analyzed by western blot. We couldn't obtain consistent western blot result to confirm the

protein knockdown. Even in our control samples, proteins of interest (DUSP11, DXO, DCP2, and NUDT2) were not detected consistently. Several adjustments were tried to improve western blot consistency, from testing primary antibodies from different suppliers or using different detection methods such as chemiluminescent or fluorescent antibodies. None have been able to produce results that we expected. Fortunately, we were able to get confirmation of RNA level reductions for each RNA decay gene (Fig. 9). DUSP11 siRNA treatment showed a reduction of RNA level to 14% compared to the control after 48 hours post infection.

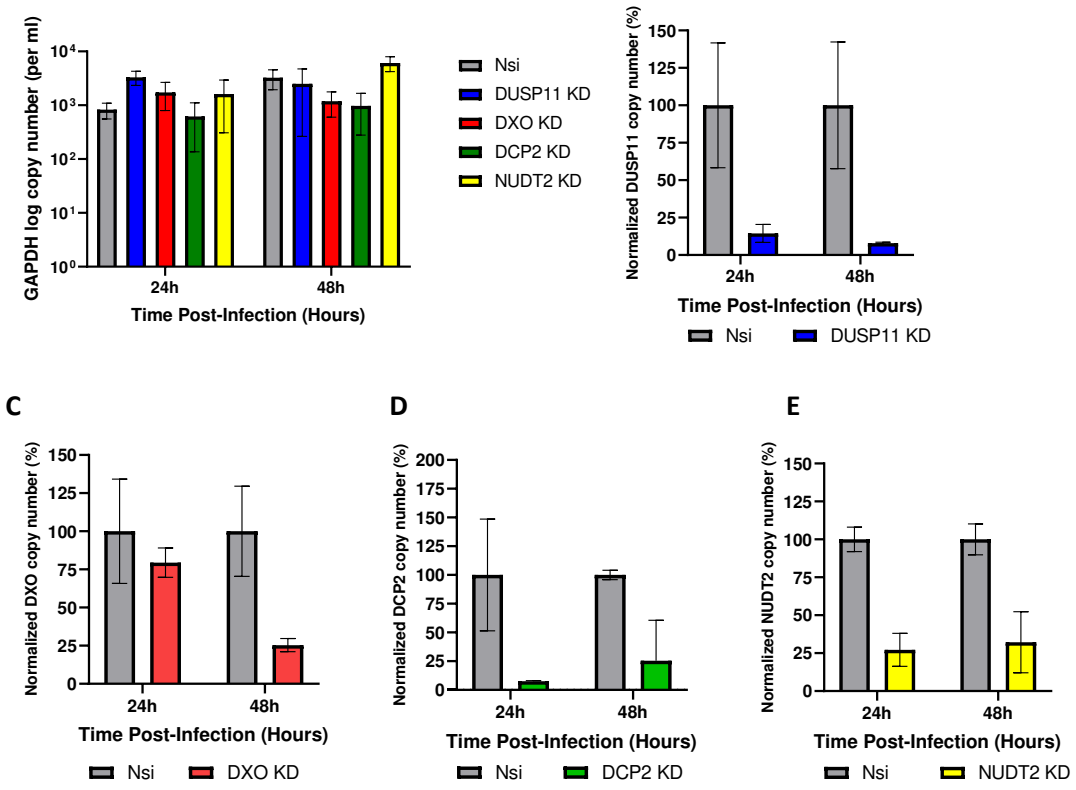

Fig. 9 ***Confirmation of RNA decay proteins knockdown using digital droplet PCR.*** Huh7 cells were transfected with respective siRNA and after 48 hours were infected with WNV (MOI = 0.01). Cells were harvested at 24 hours and 48 hours post infection and total cellular RNA were extracted and used as template for digital droplet PCR (ddPCR). (a) GAPDH level was quantified and used to normalize the copy number for other proteins. (b) to (e) showed the reduction of gene copy number compared to Neg siRNA control (Nsi) in percent (%). Results were obtained from two independent experiments and error bars represent standard error calculated from the mean.

DCP2 and NUDT2 RNA level drops from 100% to 25% and 32% respectively. DXO knockdown showed to be the least effective at 24 hours post infection. Although at 48 hours post infection, it manages to drop the RNA level to 25% compared to the control. These data suggested that siRNA transfection successfully lowered the mRNA levels of RNA decay proteins at 48 hours post infection in WNV infected cells.

4. DCP2 siRNA knockdown decreases the production of intracellular and extracellular WNV RNA.

Both intracellular and extracellular WNV RNA production were assessed in cells that are depleted of RNA decay proteins. Based on the ddPCR result we obtained, at 24 hours post infection, no significant differences were observed in the intracellular and extracellular level of viral RNA (Fig. 10a & c). At 48 hours post infection, knockdown of DUSP11 and NUDT2 did not show any major difference in terms of viral RNA production intracellularly or extracellularly when compared to its control (Fig. 10b & d). Surprisingly, these are not aligned with our previous finding in the replicon system. The difference between authentic virus vs replicon system can be caused by several factors such as replicon construct that is lacking in structural proteins and different compartmentalization of virus infection vs replicon transfection. Interestingly, knockdown of DCP2 caused lower production of WNV RNA both from intracellular and extracellular samples (Fig. 10b &d). This is aligned with our result from replicon system and both these data suggest that DCP2 seems to help and support the replication of WNV.

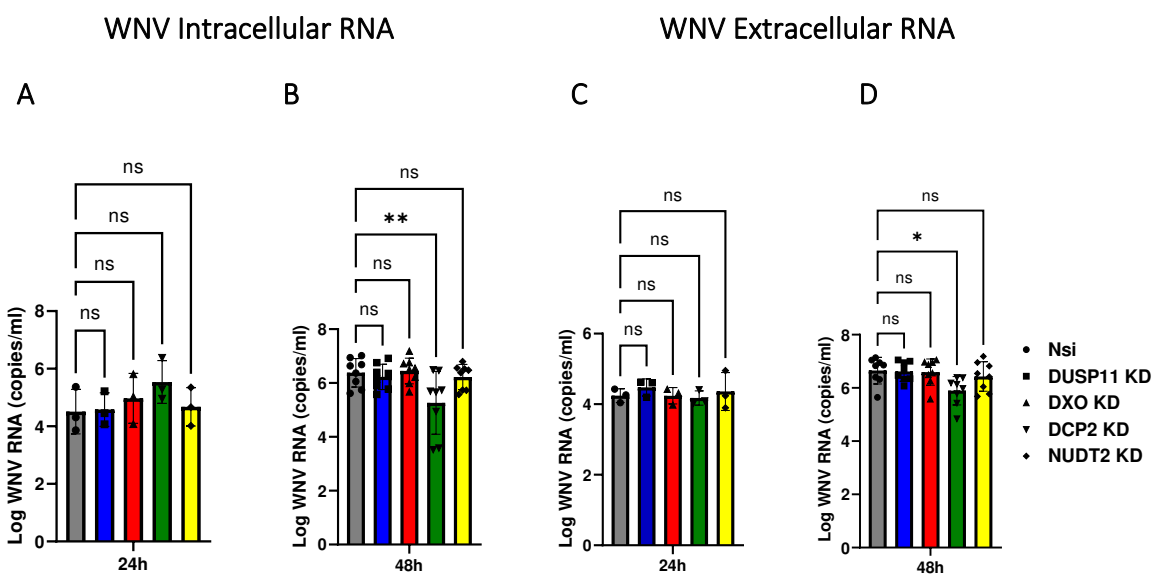

Fig. 10 ***DCP2 depletion decrease the production of West Nile virus intracellular and extracellular RNA at 48 hours post infection.*** Huh7 cells were transfected with different siRNAs and then further infected with WNV at MOI of 0.01. After 24- and 48-hours cells and supernatants were harvested and subjected to RNA isolation. RNA from cells were used to measure the production of intracellular WNV RNA (a) and (b). Supernatants were used to measure extracellular viral RNA production using ddPCR (c) and (d). Data were collected from multiple independent experiments and error bars represent standard deviation from the population. Significant results were obtained from one-way ANOVA statistical analysis with * p <0.05 and ** p<0.01.

To investigate the effect of RNA decay proteins during West Nile virus infection, Huh7 cells were transfected with siRNA to deplete RNA decay proteins and these cells were further infected with West Nile virus. At 24 hours post-infection, no significant changes were observed across different RNA decay proteins knockdown cells (Fig. 11a). However, at 48 hours post-infection, in DCP2 knockdown cells significant decreases in infectious virus production were observed (Fig. 11b). Combining the observations from intracellular and extracellular WNV RNA detection, DCP2 appears to be needed not only to help produce viral RNA but also needed to produce infectious virus.

5. DCP2 siRNA knockdowns decrease the production of Zika virus intracellular RNA, extracellular RNA, and production of infectious virus.

To determine if reduction of RNA decay proteins showed consistent effect in different flaviviruses, we assessed the effect of decapping enzymes knockdown (DXO and DCP2) in ZIKV infected cells. After 48 hours, infected cells were collected and extracted RNA was used as the template for intracellular ZIKV RNA detection. Supernatants samples were also collected for extracellular virus and infectious virus quantification. Our results showed that DXO knockdown did not affect the intracellular and extracellular production of ZIKV RNA or infectious ZIKV virus (Fig. 12a & b). However, DCP2 knockdown significantly altered the production of both intracellular and extracellular ZIKV RNA (Fig. 12a & b).

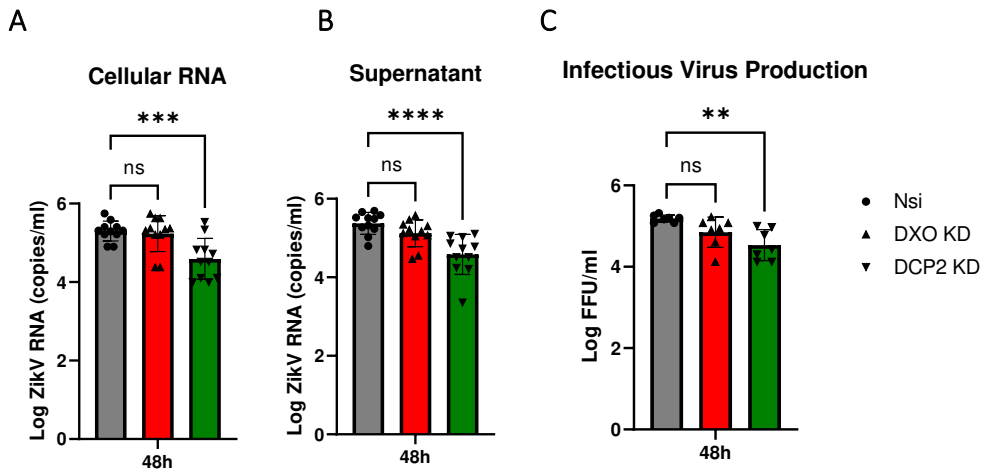

Fig. 12 ***DCP2 knockdown affect the production of Zika virus intracellular RNA, extracellular RNA, and infectious virus production.*** Huh7 cells were transfected with siRNA against DXO and DCP2. Huh7 KD cells were infected with Zika virus (MOI = 0.01) and after 48 hours post-infection total cellular and supernatant RNAs were collected. Intracellular ZIKV RNA (a) and extracellular ZIKV RNA (b) were quantified using ddPCR. Infectious virus production at 48 hours post-infection(c) was quantified using Focus forming assay. Data points were collected from multiple independent experiments. Statistical analysis was performed using one-way ANOVA test with significant result described as $p<0.05$ (** $p = 0.002$, *** $p = 0.001$, **** $p<0.001$).

DCP2 knockdown decreased the production of ZIKV RNAs by ~0.8 log compared to controls, similar to the effect observed with WNV RNAs.

Consistent effect is also observed in infectious virus production of ZIKV, knockdown of DCP2 significantly decreased the infectivity of ZIKV by ~0.6 log compared to the negative siRNA control. Collectively, DCP2 knockdown resulted in a significant reduction of viral RNA and infectivity of ZIKV, similar to what was observed with WNV.

6. DXO and DCP2 KD do not alter yellow fever virus RNA production but increase the production of infectious virus in Huh7 cells.

To compare and observe the effect of decapping enzymes in another flavivirus, yellow fever virus (strain 17D) was tested in the same fashion as WNV and ZIKV in previous experiments. Our findings showed that depleting DXO and DCP2 using siRNA do not significantly affect viral RNA production of YFV both at intracellular and extracellular level, which was different than

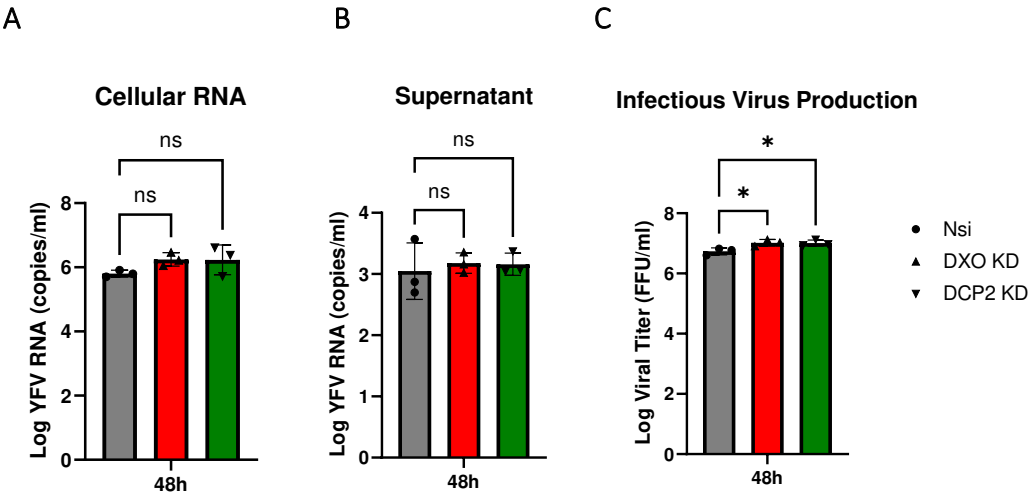

Fig. 13 ***Decapping enzymes knockdown does not alter viral RNA production but increases infectious virus production.*** Prior to infection with YFV-17 D (MOI = 0.01), Huh7 cells were transfected with siRNA targeting DXO and DCP2. 48 hours post-infection, viral RNA was detected with ddPCR (a) and (b) and infectious virus production was quantified with focus forming assay (c). Data points were collected from multiple independent experiments. Standard error bars represent standard deviation from the samples. Statistical analysis was performed using one-way ANOVA test with * $p<0.05$.

our WNV and ZIKV results (Fig. 13). However, our data suggested there is a slight increase in the viral RNA production in decapping enzymes KD cells, but it was not found to be significant. Interestingly, DXO and DCP2 KD cells showed a significantly higher infectious YFV production compared to controls, indicating that these two enzymes are antagonistic against YFV and their depletion enhanced virus particle production or infectivity. Furthermore, this is the only flavivirus we tested in this study to show that DCP2 or DXO decapping enzymes were antiviral against capped flavivirus. Collectively, our data suggested that different flaviviruses may interact differently with RNA decay pathway decapping enzymes, although the mechanism for these observed differences is not currently clear.

7. Assessing the effect of Stem-loop A structure in 5'UTR of WNV that potentially affect decapping enzyme and XRN1 sensitivity.

The results generated to this point suggest that WNV and ZIKV, but not YFV, require DCP2 for productive replication. As DCP2's function is to de-cap RNAs, we sought to develop an assay to 1) quantify the number of monophosphorylated viral RNAs produced infected wildtype and DCP2 knockdown cells and 2) begin to assess the role of the flavivirus 5' UTR, and specifically stem-loop A (SLA) in DCP2 decapping efficiency. To do this, our approach is to take advantage of the ability of monophosphorylated RNAs to be degraded by XRN1 and quantifying how enzymatic treatment of viral RNAs affects XRN1 susceptibility. We are currently developing this XRN1 sensitivity assay (Fig. 14) utilizing *in vitro* RNA transcripts with capped, triphosphate/diphosphate/monophosphate 5' ends and commercially available RNA decay pathway enzymes (human XRN1 and yeast DCP2 decapping enzymes) prior to testing authentic viral RNAs derived from infected cells to fine tune the assay.

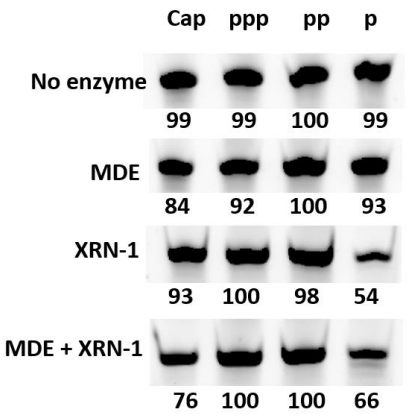

Fig. 14 ***Preliminary result of in vitro XRN1 sensitivity assay showed that XRN1 and MDE treatment resulted in partial degradation in RNA with 5' SLA structure.*** WNV 5' UTR *in vitro* transcribed RNA were synthesized in four different forms: Gppp-SLA (Cap), triphosphorylated SLA RNA (ppp), diphosphorylated SLA RNA (pp), and monophosphorylated SLA RNA (p). Enzymatic treatments were then added to different forms of RNA, the treatments are XRN1 exonuclease + mRNA decapping enzyme (MDE), XRN1 only, MDE only, and no enzyme as control. Following incubation and enzyme inactivation, samples were run in 15% urea gel and visualized with SYBR-Gold. Numbers below the image indicate band intensity compared to the control (ppp and pp-RNA).

Additionally, using *in vitro* transcripts allows for examination of the effects of RNA structures present in the viral 5' UTR (such as SLA) on decapping and XRN1 sensitivity. Our preliminary result showed that SLA-containing RNA seemed to be partially degraded when compared to the no enzyme control, although we did not see complete degradation of monophosphorylated RNA even after an hour incubation with XRNI. Capped, tri-, and di-phosphorylated are resistant to XRN1 degradation, but partial degradation of the capped RNA can be clearly observed in combined XRN1 + MDE treatment.

We are currently optimizing and synthesizing RNAs lacking the SLA to give us a better comparison of SLA-containing RNA vs RNA without SLA structure to determine if SLA alters decapping efficiency and/or XRN1 sensitivity. Overall, this preliminary result showed that SLA containing RNA can be partially degraded by RNA decay enzymes, but further analyses and assay development is needed.

DISCUSSION

The RNA decay pathway has been described to possess the capability to inhibit RNA virus replication, and many viruses develop evasion mechanisms to circumvent the effects of the pathway (54,91,92). The RNA decay pathway can be detrimental to RNA viruses and studying it may help us to develop novel strategies to stop virus replication especially for viruses with no established treatment or cure available such as Flaviviruses. The study of flaviviruses and RNA decay pathway has been limited to XRN1 exonuclease, primarily due to the production of sfRNAs by XRN1 (93). Stalling of XRN1 by the 3'UTR secondary structure in flavivirus 3' UTR RNAs has been shown to be beneficial for flaviviruses since inhibition of XRN1 increases viral RNA stability and results in disruption of host cell gene regulation (47). Additionally, mutant viruses lacking xrRNAs in the 3'UTR and incapable of forming sfRNA have been associated with lower replication rate and less cytopathic effect on cells (46). Therefore, it was known that XRN1 was important in forming sfRNAs and that XRN1 inhibition is important for flavivirus disease pathogenesis, but how substrates for XRN1 degradation are formed during infection was unclear. In this study we demonstrated the effect of different proteins related to RNA decay pathway by knocking down the proteins using siRNA and assess the effect of the knockdown on viral infectivity, intracellular RNA, and extracellular RNA production in three different flaviviruses (West Nile virus, Zika virus, and yellow fever virus), and focused on uncovering other RNA decay factors that may help provide uncapped RNAs for XRN1 degradation and inhibition.

The stalling effect of XRN1 by the 3'UTR of flavivirus can only happen when flavivirus RNA are reduced to RNA decay intermediate monophosphorylated RNA (p-RNA). The origin of

p-RNA in flavivirus replication is currently unknown. It can be assumed that p-RNA can be formed from degradation of triphosphorylated RNA (ppp-RNA) or products of decapping process since most flavivirus RNA is known to be capped. Our study focuses on two groups of proteins, triphosphatases known to reduce ppp-RNA to p-RNA such as DUSP11 and NUDT2, and decapping enzymes, DXO and DCP2. By knocking down these proteins we were able to pinpoint which proteins had an effect on viral RNA synthesis and infectious virus production. Therefore, offering a clue to how RNA decay pathway affects viral replication and possibly the origin of XRN1 substrate.

Our viability assessment of siRNA knockdown in Huh7 cells showed that no significant reduction in cell viability after 48 hours post-transfection. However, a slight reduction in viability was observed in NUDT2 KD cells. NUDT2 is not an essential gene and effort to produce knock out mouse has been previously successful (53). Furthermore, NUDT2 has also been associated with diadenosine 5′, 5‴-P1,P4-tetraphosphate (Ap4A), a cytotoxic protein closely related to DNA damage and translational stress (94). Accumulation of Ap4A is usually prevented by NUDT2 hydrolase activity. Moreover, siRNA depletion of NUDT2 have also been associated with slower cell proliferation due to the inhibitory effect of Ap4A on DNA replication initiation (95). Therefore, the reduction in cellular viability that we observed in this study may come from accumulation of cytotoxic Ap4A (94) or reduced cell growth (95). Nonetheless, we were able to incorporate the reduced cell viability into our data analysis and decouple virological readouts from knockdown effects.

To enable quick screening of RNA decay proteins knockdown on flavivirus replication, we designed an experiment using Huh7 cells that had been siRNA mediated knockdown and transfected with a WNV replicon system with luciferase reporter gene. We wanted to see if the quick and dirty system could provide a broad view of what happens with the replication of viral RNA when the cellular triphosphatases or decapping enzymes are absent. Our data suggested that DUSP11 and NUDT2 are antiviral to the replicon replication. Both proteins are triphosphatases that have been demonstrated to work against viruses that produce uncapped ppp-RNA transcripts (53,54), so this result was very interesting. Our replicon system is designed to generate capped viral RNA through Pol II mediated transcription in the nucleus, which is subsequently transported to the cytoplasm for translation and replication. DUSP11 and NUDT2 are both found in the nucleus and replicon RNA is also produced in the nucleus, raising the possibility that the replicon RNA was interacting with DUSP11 and NUDT2 in the nucleus. Therefore, DUSP11 and NUDT2 mediated degradation may occur before the co-transcriptional capping begins. Contrary to our replicon system, authentic flavivirus replication happened in the cytoplasm where the virus will travel and form a replication complex in the endoplasmic reticulum (ER). The difference in viral RNA compartments between the replicon vs authentic flavivirus provided a window for DUSP11 and NUDT2 (both localized in nucleus and cytoplasm) processing when viral RNA is present in the nucleus (53,83). This discrepancy potentially explained why DUSP11 and NUDT2 seemingly showed antiviral effect on our replicon system that is not observed with authentic virus infections.

Another possibility is that the viral structural proteins may interfere with DUSP11 and NUDT2 activity. Our WNV replicon was constructed without the structural proteins present in

infectious flaviviruses. Several phosphatases have been reported to be inhibited or sequestered by the presence of viral capsid (96), is it is possible that the effect seen with the WNV replicon system is a result to structural protein inhibition. Future experiments to examine the interaction between flavivirus structural proteins and DUSP11 or NUDT2 will help clarify interactions between these phosphatases and capsid or other structural proteins. This could be achieved using immunoprecipitation assays to co-precipitate DUSP11 or NUDT2 with flavivirus capsid, prM, or envelope proteins.

Our replicon transfection data suggested that knockdown of DXO did not affect the production of viral RNA. DXO is known to be a decapping enzyme that is specifically targeting cap structure without 2'O methylation (Cap 0) (73). Viral RNA produced by our replicon system mimic the structure of authentic flavivirus 5'cap which is Cap 1 structure that is methylated at the N7 and 2'O site. Consequently, the 2'O methylation generated by initial Pol II transcription likely reduced the affinity of DXO for the initial viral replicon RNA generated from the expression plasmid. Subsequent viral replicon replication in the cytoplasm would be generated through viral replication, and if 2'O methylation was present on capped replicon RNAs the RNA would likely be resistant to DXO. This observation is in line with our studies with infectious WNV, ZIKV, and YFV viruses. In DXO knockdown cells, production of infectious virus, intracellular RNA, and extracellular RNA were not affected compared to the control. Previously, our lab conducted a similar experiment utilizing DXO knock out cells generated with CRISPR/Cas9. The previous data our lab generated indicated that knocking out DXO affected synthesis of ZIKV RNA and production of viral titer in Kunjin virus (KUNV) and YFV (97). Although our current project did not show similar results, the difference in methods (knockout vs

knockdown) and the use of different cells (HEK293 vs Huh7) may contribute to the observed differences. We also need to consider that our siRNA knockdown is not at 100% efficiency (especially at 24-hour timepoint) meaning that there are likely residual DXO transcripts and proteins being expressed in the cells. In the future, optimizing the knockdown or knockout experiment to achieve a more efficient depletion need to be performed. Interestingly, another decapping enzyme we test in this study, which is DCP2, showed to be significantly affect viral RNA production in the replicon system and in two of the flaviviruses we tested (WNV and ZIKV).

As we validate the effect of RNA decay proteins knockdown using authentic flaviviruses, we noticed that at 24-hours post infection no significant effect in knockdown of RNA decay proteins (DUSP11, DXO, DCP2, and NUDT2) on WNV RNA and infectious virus production were observed. This observation could be caused due to the early stage of the infection where the difference in viral RNA and infectious virus were not as amplified at 48-hours post infection. Taking the sigmoidal growth curve as a model, at 24-hour time point, production of virus would lie at the very beginning where the growth curve just started to pick up and the difference between wild type cells and KD cells were present but small. However, at 48-hour time point when the infection was more established, the small difference would be amplified and provided better growth curve separation and resolution between control cells vs KD cells as to what we observed with our data.

We showed that by knocking down DCP2, infectious virus production, intracellular RNA, and extracellular RNA production in WNV and ZIKV were inhibited. These results

indicate that DCP2 is proviral and potentially important in flavivirus replication. DCP2 is a decapping enzyme that recognizes both cap 0 and cap 1 structures as substrates, releasing m7GDP and p-RNA as the products of the reaction (98). Monophosphorylated RNA (p-RNA) produced from DCP2 reaction can be further degraded by exonuclease XRN1. However, in the context of flavivirus infection, p-RNA is needed to form sfRNA for XRN1 stalling. sfRNA has been reported to contribute to the evasion of the type I Interferon response (48,99,100). The exact mechanism of how sfRNA inhibits type I interferon responses has not been fully elucidated yet. Presumably, direct interaction between sfRNA and RNA binding proteins that are stimulated by interferon activation such as RNase L, protein kinase R, and shiftless protein (SHFL) may facilitate interferon inhibition (48,101,102). Additionally, Huh7 cells have been known to possess a functional interferon response (89). Therefore, the proviral effects of DCP2 knockdown may be due to lack of sfRNA production resulting in induction of a more robust type I Interferon response. To verify this, further experiments are needed to investigate sfRNA production in DCP2 knockdown cells. This can be achieved by designing a primer that targets the 3'UTR that covers the sfRNA region. Quantification of the sfRNA can be performed using ddPCR or 3' UTR directed Northern blots can also be used to examine sfRNA production in the presence or absence of DCP2. Additionally, global analysis of transcriptomic profile of infected cells (DCP2 knockdown vs control) can also inform whether type I interferon response related genes or Interferon stimulated genes (ISGs) are upregulated or downregulated. These types of studies will help define the relationship between DCP2 and sfRNA and their impact on immune modulation during the infection. Alternatively, we hypothesize that the lack of sfRNA production in DCP2 KD cells also means that XRN1 is not getting stalled. Stalling of XRN1 can be detrimental to the cells, especially since XRN1 is also a co-regulator of gene expression.

Short-lived mRNA transcripts have been shown to be stabilized and upregulated during stalling of XRN1 in the 5'UTR region of Hepatitis C virus (HCV). Some of these short-lived transcripts belong to the proteins that regulate innate immune response, inflammatory response, transcription factors, and cell differentiation (103). Increased abundance of these mRNA dysregulates the gene regulation that can impact translation process within the cells.

DCP2 knockdown affects replication of different flaviviruses distinctly. In this study we showed that DCP2 knockdown affects WNV and ZIKV negatively but not YFV. Instead, DXO and DCP2 depletion showed a non-significant increase in intracellular YFV RNA and extracellular RNA. Considering the data trend and error bars in YFV RNA detection, we think doing more biological replicates are needed to confirm our finding. Intriguingly, DXO and DCP2 depletion resulted in significant elevation of infectious virus production. This suggest that DXO and DCP2 may both influence YFV production of infectious virus. The variation in response to DCP2 depletion could be explained by their slight differences in the genome structure particularly in their 5' UTR and 3' UTR regions. For example, WNV and Dengue virus (DENV-2) possessed two highly structured stem loop (SLA and SLB) at their 5'UTR while YFV only known to contain a single SLA structure (104). Variations in the 5'UTR region may influence YFV RNA sensitivity to decapping enzymes, although this has not been examined. Interestingly, increased sensitivity to decapping enzymes should correlate to the production of sfRNA and increased stalling of XRN1. Therefore, the antiviral effect of DCP2 in YFV is unexpected. Unfortunately, since we do not measure the production of sfRNA in this study it is not possible to conclude whether antiviral effect exhibited by DCP2 KD is caused by a slightly more effective 5'-3' XRN1 mediated decay or by other unknown mechanism. Another plausible explanation is

that YFV has been shown to produce two forms of sfRNA, the larger known as sfRNA1 and the smaller known as sfRNA2 (105). sfRNA2 contains a smaller 3' end compared to sfRNA1 and has been hypothesized to undergo additional processing or processed by the 3'-5' RNA decay pathway as sfRNA2 is not found in the insect cells where 5'-3' RNA decay pathway is more dominant (105). Knocking down DCP2 may redirect the RNA decay pathway from the 5'-3' to 3'-5' pathway where its potentially less beneficial for YFV. Further studies are needed to confirm DCP2 role on YFV replication. Firstly, quantifying the amount of sfRNA produced after infection may tell us whether the antiviral effect of DCP2 is correlated with reduction of sfRNA production. Secondly, it is worth investigating the effect of 3'-5' RNA decay pathway in YFV replication. This can be achieved by generating cells that are deficient of DcpS (decapping enzymes for 3'-5' RNA decay pathway) and exosome (exoribonuclease for 3'-5' RNA decay pathway). These cells would then be infected with YFV and analyzed their intracellular RNA, extracellular RNA, and infectious virus production.

There are limitations in our study as we are we only examined proteins in 5'-3' RNA decay pathway. Multiple RNA decay pathway exists (e.g., 3'-5' RNA decay pathway and endonuclease mediated RNA decay pathway) and there are obviously many more proteins, cofactors, and enzymes that are equally involved in the RNA decay pathway. For example, NUDT16 and NUDT3 are also decapping enzymes involved in regulating mRNA stability within our cells (68). Some of these decapping enzymes (such as DCP2 and NUDT16) shared common substrate (m7Gppp cap) and may contribute to functional redundancy that will be worth investigating. Similar thing is also observed in the triphosphatases that analyzed in this study, DUSP11 and NUDT2. Both enzymes have similar mechanism of action and presumably fulfill

redundant function within our cells. This may explain why we couldn't observe any significant difference when we knockdown only one of the proteins. We would also need to address that the siRNA mediated knockdown experiments that we conducted in this study are not 100% efficient. Although we were able to deplete the RNA transcripts of our target protein up to ~70-80% compared to the control, some spillover translation can still occur. Therefore, in the future doing a knockout experiment by using the CRISPR/Cas9 knockouts or haploid knock out cell lines (Hap1 cells) will allow us to compare and possibly complete generate more complete data than we obtained in this study.

We are currently in the process of optimizing an in vitro XRN1 sensitivity assay where we will analyze in vitro transcribed RNA of 5'UTR of flavivirus and total RNA from infected cells using enzymatic treatment of commercially available decapping enzymes (NEB MDE, yeast DCP-1/DCP2) and human XRN1. This assay is intended to assess how DCP2 interacts with the 5'UTR of flavivirus RNA and whether secondary present (SLA) in the 5'UTR affect the decapping process or not. If decapping occurs with RNAs lacking SLA but not with RNA containing the SLA, then it will tell us that DCP2-mediated decapping may happen earlier during the transcription process where the secondary structure has not been formed yet (Fig. 15). Our preliminary result showed that combined enzymatic treatment of MDE and XRN1 in RNA with SLA at the 5'UTR showed partial degradation compared to its control. However, since we do not yet have the data for RNA without secondary structure at the 5'UTR, it is too early to conclude that the SLA structure inhibits DCP2 activity or not. Currently, we are in the process of synthesizing the 5' UTR RNAs without SLA and will subject these RNA into the same enzymatic treatment.

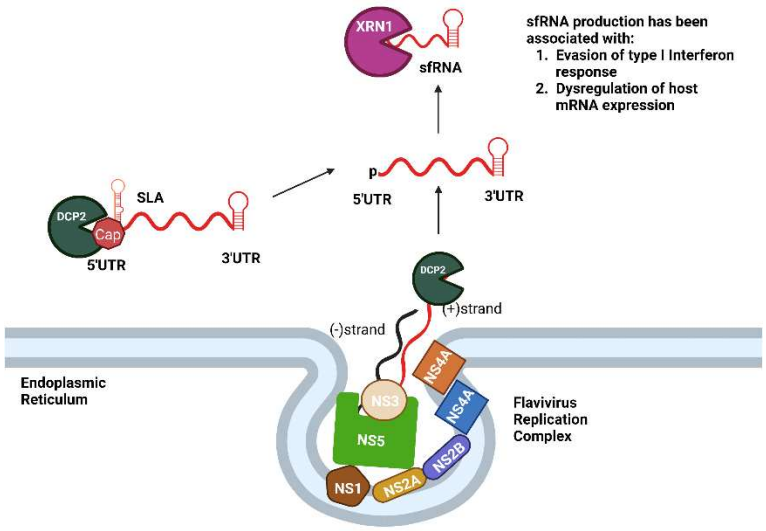

Fig. 15 ***Proposed DCP2 mechanism of action within flavivirus infected cells.*** DCP2 potentially affect decapping of viral RNA in several fashions. Decapping of viral RNA can happen when fully capped viral RNA containing SLA structure in the cytoplasm or during early stage of viral RNA synthesis that still lacks the SLA structure in the replication complex. Decapped viral RNA (p-RNA) will then be degraded by XRN1 exonuclease. Image generated with BioRender.

Overall, based on our siRNA mediated knockdown experiments, we observed that a specific RNA decay pathway enzyme, DCP2, can positively or negatively affect flavivirus replication depending on the virus in question. Our data suggested that RNA triphosphatases DUSP11 and NUDT2 did not affect WNV replication. However, we have not tested these proteins in other flaviviruses yet. Future research examining the role of RNA triphosphatases in different flaviviruses may show potential effect on their replication, especially since DUSP11 has been shown to be effective in reducing replication of the ppp-RNA producing HCV (54). We also demonstrated that knocking down decapping enzyme, DCP2 inhibit the intracellular RNA, extracellular RNA, and infectious virus production in WNV and ZIKV but not in YFV. These data suggested that DCP2 is proviral for some flaviviruses. Additionally, our data showed that different flavivirus seems to have different sensitivity or outcome from DCP2 decapping activity. Specifically, since DCP2 is tightly linked with XRN1 mediated decay pathway and

sfRNA production in flavivirus, it would be interesting to expand our current findings to see the relationship between DCP2 and sfRNA production. Therefore, the data that we collected can hopefully stimulate more research on DCP2 effect on other viruses.

REFERENCES

1. Thompson R, Martin Del Campo J, Constenla D. A review of the economic evidence of Aedes-borne arboviruses and Aedes-borne arboviral disease prevention and control strategies. Expert Rev Vaccines. 2020 Feb 1;19(2):143–62.

2. Daep CA, Muñoz-Jordán JL, Eugenin EA. Flaviviruses, an expanding threat in public health: focus on Dengue, West Nile, and Japanese encephalitis virus. J Neurovirol. 2014 Dec;20(6):539–60.

3. Colón-González FJ, Sewe MO, Tompkins AM, Sjödin H, Casallas A, Rocklöv J, et al. Projecting the risk of mosquito-borne diseases in a warmer and more populated world: a multi-model, multi-scenario intercomparison modelling study. Lancet Planet Health. 2021 Jul 1;5(7):e404–14.

4. Gan SJ, Leong YQ, bin Barhanuddin MFH, Wong ST, Wong SF, Mak JW, et al. Dengue fever and insecticide resistance in Aedes mosquitoes in Southeast Asia: a review. Parasit Vectors. 2021 Jun 10;14(1):315.

5. Edenborough KM, Flores HA, Simmons CP, Fraser JE. Using Wolbachia to Eliminate Dengue: Will the Virus Fight Back? J Virol. 2021 Jun 10;95(13):e02203-20.

6. Chancey C, Grinev A, Volkova E, Rios M. The Global Ecology and Epidemiology of West Nile Virus. BioMed Res Int. 2015;2015:376230.

7. Ronca SE, Ruff JC, Murray KO. A 20-year historical review of West Nile virus since its initial emergence in North America: Has West Nile virus become a neglected tropical disease? PLoS Negl Trop Dis. 2021 May 6;15(5):e0009190.

8. Cho H, Diamond MS. Immune responses to West Nile virus infection in the central nervous system. Viruses. 2012 Dec 17;4(12):3812–30.

9. Petersen LR, Brault AC, Nasci RS. West Nile Virus: Review of the Literature. JAMA. 2013 Jul 17;310(3):308–15.

10. Lee HJ, Longnecker M, Calkins TL, Renfro AD, Fredregill CL, Debboun M, et al. Detection of the Nav channel kdr-like mutation and modeling of factors affecting survivorship of Culex quinquefasciatus mosquitoes from six areas of Harris County (Houston), Texas, after permethrin field-cage tests. PLoS Negl Trop Dis. 2020 Nov 19;14(11):e0008860.

11. Dodson BL, Hughes GL, Paul O, Matacchiero AC, Kramer LD, Rasgon JL. Wolbachia enhances West Nile virus (WNV) infection in the mosquito Culex tarsalis. PLoS Negl Trop Dis. 2014 Jul;8(7):e2965.

12. Song BH, Yun SI, Woolley M, Lee YM. Zika virus: History, epidemiology, transmission, and clinical presentation. J Neuroimmunol. 2017 Jul 15;308:50–64.

13. Wikan N, Smith DR. Zika virus: history of a newly emerging arbovirus. Lancet Infect Dis. 2016 Jul 1;16(7):e119–26.

14. Oehler E, Watrin L, Larre P, Leparc-Goffart I, Lastere S, Valour F, et al. Zika virus infection complicated by Guillain-Barre syndrome--case report, French Polynesia, December 2013. Euro Surveill Bull Eur Sur Mal Transm Eur Commun Dis Bull. 2014 Mar 6;19(9):20720.

15. Kleber de Oliveira W, Cortez-Escalante J, De Oliveira WTGH, do Carmo GMI, Henriques CMP, Coelho GE, et al. Increase in Reported Prevalence of Microcephaly in Infants Born to Women Living in Areas with Confirmed Zika Virus Transmission During the First Trimester of Pregnancy - Brazil, 2015. MMWR Morb Mortal Wkly Rep. 2016 Mar 11;65(9):242–7.

16. França GVA, Schuler-Faccini L, Oliveira WK, Henriques CMP, Carmo EH, Pedi VD, et al. Congenital Zika virus syndrome in Brazil: a case series of the first 1501 livebirths with complete investigation. The Lancet. 2016 Aug 27;388(10047):891–7.

17. Magnus MM, Espósito DLA, Costa VA da, Melo PS de, Costa-Lima C, Fonseca BAL da, et al. Risk of Zika virus transmission by blood donations in Brazil. Hematol Transfus Cell Ther. 2018;40(3):250–4.

18. Foy BD, Kobylinski KC, Foy JLC, Blitvich BJ, Travassos da Rosa A, Haddow AD, et al. Probable Non–Vector-borne Transmission of Zika Virus, Colorado, USA. Emerg Infect Dis. 2011 May;17(5):880–2.

19. Rice ME, Galang RR, Roth NM, Ellington SR, Moore CA, Valencia-Prado M, et al. Vital Signs: Zika-Associated Birth Defects and Neurodevelopmental Abnormalities Possibly Associated with Congenital Zika Virus Infection — U.S. Territories and Freely Associated States, 2018. Morb Mortal Wkly Rep. 2018 Aug 10;67(31):858–67.

20. Freitas DA, Souza-Santos R, Carvalho LMA, Barros WB, Neves LM, Brasil P, et al. Congenital Zika syndrome: A systematic review. PLoS ONE. 2020 Dec 15;15(12):e0242367.

21. do Rosário MS, de Jesus PAP, Vasilakis N, Farias DS, Novaes MAC, Rodrigues SG, et al. Guillain–Barré Syndrome after Zika Virus Infection in Brazil. Am J Trop Med Hyg. 2016 Nov 2;95(5):1157–60.

22. Pattnaik A, Sahoo BR, Pattnaik AK. Current Status of Zika Virus Vaccines: Successes and Challenges. Vaccines. 2020 May 31;8(2):266.

23. Byrne AB, Talarico LB. Role of the complement system in antibody-dependent enhancement of flavivirus infections. Int J Infect Dis. 2021 Feb 1;103:404–11.

24. Katzelnick LC, Narvaez C, Arguello S, Mercado BL, Collado D, Ampie O, et al. Zika virus infection enhances future risk of severe dengue disease. Science. 2020 Aug 28;369(6507):1123–8.

25. Olímpio FA, Falcão LFM, Carvalho MLG, da Costa Lopes J, Mendes CCH, Filho AJM, et al. Endothelium Activation during Severe Yellow Fever Triggers an Intense Cytokine-Mediated Inflammatory Response in the Liver Parenchyma. Pathogens. 2022 Jan 15;11(1):101.

26. Frierson JG. The Yellow Fever Vaccine: A History. Yale J Biol Med. 2010 Jun;83(2):77–85.

27. Chen LH, Wilson ME. Yellow fever control: current epidemiology and vaccination strategies. Trop Dis Travel Med Vaccines. 2020 Jan 10;6(1):1.

28. Staples JE, Barrett ADT, Wilder-Smith A, Hombach J. Review of data and knowledge gaps regarding yellow fever vaccine-induced immunity and duration of protection. Npj Vaccines. 2020 Jul 6;5(1):1–7.

29. Montalvo Zurbia-Flores G, Rollier CS, Reyes-Sandoval A. Re-thinking yellow fever vaccines: fighting old foes with new generation vaccines. Hum Vaccines Immunother. 2022 Jan 31;18(1):1895644.

30. Laureti M, Narayanan D, Rodriguez-Andres J, Fazakerley JK, Kedzierski L. Flavivirus Receptors: Diversity, Identity, and Cell Entry. Front Immunol. 2018 Sep 26;9:2180.

31. Chao LH, Klein DE, Schmidt AG, Peña JM, Harrison SC. Sequential conformational rearrangements in flavivirus membrane fusion. eLife. 3:e04389.

32. Gillespie LK, Hoenen A, Morgan G, Mackenzie JM. The Endoplasmic Reticulum Provides the Membrane Platform for Biogenesis of the Flavivirus Replication Complex. J Virol. 2010 Oct;84(20):10438–47.

33. Ngo AM, Shurtleff MJ, Popova KD, Kulsuptrakul J, Weissman JS, Puschnik AS. The ER membrane protein complex is required to ensure correct topology and stable expression of flavivirus polyproteins. eLife. 8:e48469.

34. Kaufusi PH, Kelley JF, Yanagihara R, Nerurkar VR. Induction of Endoplasmic Reticulum-Derived Replication-Competent Membrane Structures by West Nile Virus Non-Structural Protein 4B. PLoS ONE. 2014 Jan 20;9(1):e84040.

35. Liu L, Dong H, Chen H, Zhang J, Ling H, Li Z, et al. Flavivirus RNA cap methyltransferase: structure, function, and inhibition. Front Biol. 2010 Aug 1;5(4):286–303.

36. Galloway A, Cowling VH. mRNA cap regulation in mammalian cell function and fate. Biochim Biophys Acta Gene Regul Mech. 2019 Mar;1862(3):270–9.

37. Rouha H, Hoenninger VM, Thurner C, Mandl CW. Mutational analysis of three predicted 5′-proximal stem-loop structures in the genome of tick-borne encephalitis virus indicates different roles in RNA replication and translation. Virology. 2011 Aug 15;417(1):79–86.

38. Youn S, Li T, McCune BT, Edeling MA, Fremont DH, Cristea IM, et al. Evidence for a Genetic and Physical Interaction between Nonstructural Proteins NS1 and NS4B That Modulates Replication of West Nile Virus. J Virol. 2012 Jul;86(13):7360–71.

39. Carpio KL, Barrett ADT. Flavivirus NS1 and Its Potential in Vaccine Development. Vaccines. 2021 Jun 9;9(6):622.

40. Conde JN, Silva EM, Barbosa AS, Mohana-Borges R. The Complement System in Flavivirus Infections. Front Microbiol. 2017;8:213.

41. Edeling MA, Diamond MS, Fremont DH. Structural basis of Flavivirus NS1 assembly and antibody recognition. Proc Natl Acad Sci U S A. 2014 Mar 18;111(11):4285–90.

42. Zuo Z, Liew OW, Chen G, Chong PCJ, Lee SH, Chen K, et al. Mechanism of NS2B-Mediated Activation of NS3pro in Dengue Virus: Molecular Dynamics Simulations and Bioassays. J Virol. 2009 Jan;83(2):1060–70.

43. Klaitong P, Smith DR. Roles of Non-Structural Protein 4A in Flavivirus Infection. Viruses. 2021 Oct 15;13(10):2077.

44. Issur M, Geiss BJ, Bougie I, Picard-Jean F, Despins S, Mayette J, et al. The flavivirus NS5 protein is a true RNA guanylyltransferase that catalyzes a two-step reaction to form the RNA cap structure. RNA. 2009 Dec;15(12):2340–50.

45. Zhou Y, Ray D, Zhao Y, Dong H, Ren S, Li Z, et al. Structure and function of flavivirus NS5 methyltransferase. J Virol. 2007 Apr;81(8):3891–903.

46. Pijlman GP, Funk A, Kondratieva N, Leung J, Torres S, van der Aa L, et al. A Highly Structured, Nuclease-Resistant, Noncoding RNA Produced by Flaviviruses Is Required for Pathogenicity. Cell Host Microbe. 2008 Dec 11;4(6):579–91.

47. Moon SL, Anderson JR, Kumagai Y, Wilusz CJ, Akira S, Khromykh AA, et al. A noncoding RNA produced by arthropod-borne flaviviruses inhibits the cellular exoribonuclease XRN1 and alters host mRNA stability. RNA. 2012 Nov;18(11):2029–40.

48. Schuessler A, Funk A, Lazear HM, Cooper DA, Torres S, Daffis S, et al. West Nile Virus Noncoding Subgenomic RNA Contributes to Viral Evasion of the Type I Interferon-Mediated Antiviral Response. J Virol. 2012 May;86(10):5708–18.

49. Ghosh S, Jacobson A. RNA decay modulates gene expression and controls its fidelity. WIREs RNA. 2010;1(3):351–61.

50. Łabno A, Tomecki R, Dziembowski A. Cytoplasmic RNA decay pathways - Enzymes and mechanisms. Biochim Biophys Acta BBA - Mol Cell Res. 2016 Dec 1;1863(12):3125–47.

51. Garneau NL, Wilusz J, Wilusz CJ. The highways and byways of mRNA decay. Nat Rev Mol Cell Biol. 2007 Feb;8(2):113–26.

52. Nickless A, Bailis JM, You Z. Control of gene expression through the nonsense-mediated RNA decay pathway. Cell Biosci. 2017 May 19;7(1):26.

53. Laudenbach BT, Krey K, Emslander Q, Andersen LL, Reim A, Scaturro P, et al. NUDT2 initiates viral RNA degradation by removal of 5′-phosphates. Nat Commun. 2021 Nov 25;12(1):6918.

54. Kincaid RP, Lam VL, Chirayil RP, Randall G, Sullivan CS. RNA triphosphatase DUSP11 enables exonuclease XRN-mediated restriction of hepatitis C virus. Proc Natl Acad Sci U S A. 2018 Aug 7;115(32):8197–202.

55. Chen CYA, Shyu AB. Mechanisms of deadenylation-dependent decay. Wiley Interdiscip Rev RNA. 2011;2(2):167–83.

56. van Eenennaam H, Jarrous N, van Venrooij WJ, Pruijn GJ. Architecture and function of the human endonucleases RNase P and RNase MRP. IUBMB Life. 2000 Apr;49(4):265–72.

57. Hollien J, Weissman JS. Decay of endoplasmic reticulum-localized mRNAs during the unfolded protein response. Science. 2006 Jul 7;313(5783):104–7.

58. Pastori RL, Schoenberg DR. The nuclease that selectively degrades albumin mRNA in vitro associates with Xenopus liver polysomes through the 80S ribosome complex. Arch Biochem Biophys. 1993 Sep;305(2):313–9.

59. Yoshida A, Ueda T. Human AP endonuclease possesses a significant activity as major 3'-5' exonuclease in human leukemia cells. Biochem Biophys Res Commun. 2003 Oct 17;310(2):522–8.

60. Huntzinger E, Kashima I, Fauser M, Saulière J, Izaurralde E. SMG6 is the catalytic endonuclease that cleaves mRNAs containing nonsense codons in metazoan. RNA N Y N. 2008 Dec;14(12):2609–17.

61. Matsushita K, Takeuchi O, Standley DM, Kumagai Y, Kawagoe T, Miyake T, et al. Zc3h12a is an RNase essential for controlling immune responses by regulating mRNA decay. Nature. 2009 Apr 30;458(7242):1185–90.

62. Tourrière H, Gallouzi IE, Chebli K, Capony JP, Mouaikel J, van der Geer P, et al. RasGAP-associated endoribonuclease G3Bp: selective RNA degradation and phosphorylation-dependent localization. Mol Cell Biol. 2001 Nov;21(22):7747–60.

63. Ramos-Lorente S, Romero-López C, Berzal-Herranz A. Information Encoded by the Flavivirus Genomes beyond the Nucleotide Sequence. Int J Mol Sci. 2021 Apr 3;22(7):3738.

64. Fontaine KA, Leon KE, Khalid MM, Tomar S, Jimenez-Morales D, Dunlap M, et al. The Cellular NMD Pathway Restricts Zika Virus Infection and Is Targeted by the Viral Capsid Protein. mBio. 2018 Nov 6;9(6):e02126-18.

65. Li M, Johnson JR, Truong B, Kim G, Weinbren N, Dittmar M, et al. Identification of Antiviral Roles for the Exon-Junction Complex and Nonsense-Mediated Decay in Flaviviral Infection. Nat Microbiol. 2019 Jun;4(6):985–95.

66. Mazeaud C, Freppel W, Chatel-Chaix L. The Multiples Fates of the Flavivirus RNA Genome During Pathogenesis. Front Genet. 2018 Dec 4;9:595.

67. Nagarajan VK, Jones CI, Newbury SF, Green PJ. XRN 5'→3' exoribonucleases: Structure, mechanisms and functions. Biochim Biophys Acta. 2013;1829(0):590–603.

68. Grudzien-Nogalska E, Kiledjian M. New Insights into Decapping Enzymes and Selective mRNA Decay. Wiley Interdiscip Rev RNA. 2017 Jan;8(1):10.1002/wrna.1379.

69. Burke JM, Kincaid RP, Nottingham RM, Lambowitz AM, Sullivan CS. DUSP11 activity on triphosphorylated transcripts promotes Argonaute association with noncanonical viral microRNAs and regulates steady-state levels of cellular noncoding RNAs. Genes Dev. 2016 Sep 15;30(18):2076–92.

70. Audic Y, Hartley RS. Post-transcriptional regulation in cancer. Biol Cell. 2004 Sep 1;96(7):479–98.

71. Li Y, Dai J, Song M, Fitzgerald-Bocarsly P, Kiledjian M. Dcp2 Decapping Protein Modulates mRNA Stability of the Critical Interferon Regulatory Factor (IRF) IRF-7. Mol Cell Biol. 2012 Mar;32(6):1164–72.

72. Mang GM, Pradervand S, Du NH, Arpat AB, Preitner F, Wigger L, et al. A neuron-specific deletion of the microRNA-processing enzyme DICER induces severe but transient obesity in mice. PloS One. 2015;10(1):e0116760.

73. Picard-Jean F, Brand C, Tremblay-Létourneau M, Allaire A, Beaudoin MC, Boudreault S, et al. 2'-O-methylation of the mRNA cap protects RNAs from decapping and degradation by DXO. PLOS ONE. 2018 Mar 30;13(3):e0193804.

74. Pan S, Li KE, Huang W, Zhong H, Wu H, Wang Y, et al. Arabidopsis DXO1 possesses deNADding and exonuclease activities and its mutation affects defense-related and photosynthetic gene expression. J Integr Plant Biol. 2020 Jul;62(7):967–83.

75. Zhou D, Lai M, Luo A, Yu CY. An RNA Metabolism and Surveillance Quartet in the Major Histocompatibility Complex. Cells. 2019 Aug 30;8(9):E1008.

76. Mugridge JS, Gross JD. Judge, Jury and Executioner: DXO functions as a decapping enzyme and exoribonuclease in pre-mRNA quality control. Mol Cell. 2013 Apr 11;50(1):2–4.

77. Lynch ER. DXO decapping exonuclease is a restriction factor for RNA viruses, The [Thesis]. Colorado State University; 2018.

78. Sikorski PJ, Warminski M, Kubacka D, Ratajczak T, Nowis D, Kowalska J, et al. The identity and methylation status of the first transcribed nucleotide in eukaryotic mRNA 5′ cap modulates protein expression in living cells. Nucleic Acids Res. 2020 Feb 28;48(4):1607–26.

79. Hopkins KC, McLane LM, Maqbool T, Panda D, Gordesky-Gold B, Cherry S. A genome-wide RNAi screen reveals that mRNA decapping restricts bunyaviral replication by limiting the pools of Dcp2-accessible targets for cap-snatching. Genes Dev. 2013 Jul 1;27(13):1511–25.

80. Li Y, Dai J, Song M, Fitzgerald-Bocarsly P, Kiledjian M. Dcp2 Decapping Protein Modulates mRNA Stability of the Critical Interferon Regulatory Factor (IRF) IRF-7. Mol Cell Biol. 2012 Mar;32(6):1164–72.

81. Deshpande T, Takagi T, Hao L, Buratowski S, Charbonneau H. Human PIR1 of the protein-tyrosine phosphatase superfamily has RNA 5'-triphosphatase and diphosphatase activities. J Biol Chem. 1999 Jun 4;274(23):16590–4.

82. Choi JH, Sullivan CS. DUSP11 and triphosphate RNA balance during virus infection. PLOS Pathog. 2021 Jan 14;17(1):e1009145.

83. Burke JM, Sullivan CS. DUSP11 - An RNA phosphatase that regulates host and viral non-coding RNAs in mammalian cells. RNA Biol. 2017 Nov 2;14(11):1457–65.

84. Choi JH, Burke JM, Szymanik KH, Nepal U, Battenhouse A, Lau JT, et al. DUSP11-mediated control of 5′-triphosphate RNA regulates RIG-I sensitivity. Genes Dev. 2020 Dec 1;34(23–24):1697–712.

85. Zhao Y, Ye X, Dunker W, Song Y, Karijolich J. RIG-I like receptor sensing of host RNAs facilitates the cell-intrinsic immune response to KSHV infection. Nat Commun. 2018 Nov 19;9:4841.

86. Song MG, Bail S, Kiledjian M. Multiple Nudix family proteins possess mRNA decapping activity. RNA N Y N. 2013 Mar;19(3):390–9.

87. Pierson TC, Sánchez MD, Puffer BA, Ahmed AA, Geiss BJ, Valentine LE, et al. A rapid and quantitative assay for measuring antibody-mediated neutralization of West Nile virus infection. Virology. 2006 Mar 1;346(1):53–65.

88. Weger-Lucarelli J, Duggal NK, Bullard-Feibelman K, Veselinovic M, Romo H, Nguyen C, et al. Development and Characterization of Recombinant Virus Generated from a New World Zika Virus Infectious Clone. J Virol. 2017 Jan 1;91(1):e01765-16.

89. Theiler M, Smith HH. The Use of Yellow Fever virus modified by in vitro cultivation for Human Immunization. J Exp Med. 1937 May 31;65(6):787–800.

90. Du Pont KE, Davidson RB, McCullagh M, Geiss BJ. Motif V regulates energy transduction between the flavivirus NS3 ATPase and RNA-binding cleft. J Biol Chem. 2020 Feb 7;295(6):1551–64.

91. Hogg JR. Viral Evasion and Manipulation of Host RNA Quality Control Pathways. J Virol. 2016 Jul 27;90(16):7010–8.

92. Molleston JM, Cherry S. Attacked from All Sides: RNA Decay in Antiviral Defense. Viruses. 2017 Jan 4;9(1):2.

93. Dilweg IW, Savina A, Köthe S, Gultyaev AP, Bredenbeek PJ, Olsthoorn RCL. All genera of Flaviviridae host a conserved Xrn1-resistant RNA motif. RNA Biol. 18(12):2321–9.

94. Marriott AS, Copeland NA, Cunningham R, Wilkinson MC, McLennan AG, Jones NJ. Diadenosine 5′, 5‴-P1,P4-tetraphosphate (Ap4A) is synthesized in response to DNA damage and inhibits the initiation of DNA replication. DNA Repair. 2015 Sep 1;33:90–100.

95. Oka K, Suzuki T, Onodera Y, Miki Y, Takagi K, Nagasaki S, et al. Nudix-type motif 2 in human breast carcinoma: A potent prognostic factor associated with cell proliferation. Int J Cancer. 2011;128(8):1770–82.

96. Airo AM, Urbanowski MD, Lopez-Orozco J, You JH, Skene-Arnold TD, Holmes C, et al. Expression of flavivirus capsids enhance the cellular environment for viral replication by activating Akt-signalling pathways. Virology. 2018 Mar 1;516:147–57.

97. Lynch ER. DXO decapping exonuclease is a restriction factor for RNA viruses. Colorado State University; 2018. Available from: https://mountainscholar.org/handle/10217/199776

98. Drazkowska K, Tomecki R, Warminski M, Baran N, Cysewski D, Depaix A, et al. 2′-O-Methylation of the second transcribed nucleotide within the mRNA 5′ cap impacts the protein production level in a cell-specific manner and contributes to RNA immune evasion. Nucleic Acids Res. 2022 Sep 9;50(16):9051–71.

99. Donald CL, Brennan B, Cumberworth SL, Rezelj VV, Clark JJ, Cordeiro MT, et al. Full Genome Sequence and sfRNA Interferon Antagonist Activity of Zika Virus from Recife, Brazil. PLoS Negl Trop Dis. 2016 Oct 5;10(10):e0005048.

100. Castro-Jiménez TK, Gómez-Legorreta LC, López-Campa LA, Martínez-Torres V, Alvarado-Silva M, Posadas-Mondragón A, et al. Variability in Susceptibility to Type I Interferon Response and Subgenomic RNA Accumulation Between Clinical Isolates of Dengue and Zika Virus From Oaxaca Mexico Correlate With Replication Efficiency in Human Cells and Disease Severity. Front Cell Infect Microbiol. 2022;12:890750.

101. Hanners NW, Mar KB, Boys IN, Eitson JL, De La Cruz-Rivera PC, Richardson RB, et al. Shiftless inhibits flavivirus replication in vitro and is neuroprotective in a mouse model of Zika virus pathogenesis. Proc Natl Acad Sci. 2021 Dec 7;118(49):e2111266118.

102. Samuel MA, Whitby K, Keller BC, Marri A, Barchet W, Williams BRG, et al. PKR and RNase L Contribute to Protection against Lethal West Nile Virus Infection by Controlling Early Viral Spread in the Periphery and Replication in Neurons. J Virol. 2006 Jul;80(14):7009–19.

103. Moon SL, Blackinton JG, Anderson JR, Dozier MK, Dodd BJT, Keene JD, et al. XRN1 Stalling in the 5' UTR of Hepatitis C Virus and Bovine Viral Diarrhea Virus Is Associated with Dysregulated Host mRNA Stability. PLoS Pathog. 2015 Mar 6;11(3):e1004708.

104. Fernández-Sanlés A, Ríos-Marco P, Romero-López C, Berzal-Herranz A. Functional Information Stored in the Conserved Structural RNA Domains of Flavivirus Genomes. Front Microbiol. 2017;8:546.

105. Silva PAGC, Pereira CF, Dalebout TJ, Spaan WJM, Bredenbeek PJ. An RNA Pseudoknot Is Required for Production of Yellow Fever Virus Subgenomic RNA by the Host Nuclease XRN1. J Virol. 2010 Nov;84(21):11395–406.